

Review

Nano-Enhanced Phase Change Materials in Latent Heat Thermal Energy Storage Systems: A Review

Kassianne Tofani and Saeed Tiari *

Biomedical, Industrial and Systems Engineering Department, Gannon University, Erie, PA 16541, USA; tofani001@gannon.edu

* Correspondence: tiari001@gannon.edu; Tel.: +1-814-871-7046

Abstract: Latent heat thermal energy storage systems (LHTES) are useful for solar energy storage and many other applications, but there is an issue with phase change materials (PCMs) having low thermal conductivity. This can be enhanced with fins, metal foam, heat pipes, multiple PCMs, and nanoparticles (NPs). This paper reviews nano-enhanced PCM (NePCM) alone and with additional enhancements. Low, middle, and high temperature PCM are classified, and the achievements and limitations of works are assessed. The review is categorized based upon enhancements: solely NPs, NPs and fins, NPs and heat pipes, NPs with highly conductive porous materials, NPs and multiple PCMs, and nano-encapsulated PCMs. Both experimental and numerical methods are considered, focusing on how well NPs enhanced the system. Generally, NPs have been proven to enhance PCM, with some types more effective than others. Middle and high temperatures are lacking compared to low temperature, as well as combined enhancement studies. Al_2O_3 , copper, and carbon are some of the most studied NP materials, and paraffin PCM is the most common by far. Some studies found NPs to be insignificant in comparison to other enhancements, but many others found them to be beneficial. This article also suggests future work for NePCM and LHTES systems.



Citation: Tofani, K.; Tiari, S. Nano-Enhanced Phase Change Materials in Latent Heat Thermal Energy Storage Systems: A Review. *Energies* **2021**, *14*, 3821. <https://doi.org/10.3390/en14133821>

Academic Editor: Ricardo J. Bessa

Received: 8 May 2021

Accepted: 22 June 2021

Published: 25 June 2021

Publisher's Note: MDPI stays neutral with regard to jurisdictional claims in published maps and institutional affiliations.



Copyright: © 2021 by the authors. Licensee MDPI, Basel, Switzerland. This article is an open access article distributed under the terms and conditions of the Creative Commons Attribution (CC BY) license (<https://creativecommons.org/licenses/by/4.0/>).

Keywords: latent heat thermal energy storage; phase change material; nanoparticles; nano-enhanced PCM

1. Introduction to Latent Heat Thermal Energy Storage

Solar energy is a great renewable energy alternative; however, it is an intermittent energy source. At night and on overcast days, solar energy is not available. This can be solved with the use of latent heat thermal energy storage (LHTES) systems, which are dispatchable. LHTES systems rely on phase change material (PCM) to charge and discharge energy in the form of heat by melting and solidification. LHTES systems can be anything from a simple container of PCM to complex systems with various enhancements. PCM is any material that can store energy through melting and release it upon solidification. This stored energy can be dispatched in the off hours to keep a system running.

LHTES systems are just one type of thermal energy storage. Other types include sensible heat storage (SHS) and thermo-chemical storage (TCS). TCS uses materials that store and release energy through endothermic and exothermic reactions, which are called thermo-chemical materials. Some examples of these materials are potassium oxide and lead oxide. Heat is applied to the material, which breaks into two parts that are separately stored. To release the energy, they are mixed back together. This process is shown in Figure 1c. SHS uses storage media such as water, sand, or rocks to store thermal energy. The most common being water. SHS is popular because it is cheap and safe, using non-toxic materials. Temperature change is what drives SHS, as shown in Figure 1a [1].

SHS is the most common method, but latent heat is even more promising. The higher thermal storage density, large array of PCMs, and nearly isothermal behavior of LHTES systems (shown in Figure 1b) make them more convenient than the other methods [2]. This means that LHTES systems can take up less volume to store the same amount of energy

as SHS, and the stable temperature allows nearly isothermal heating/cooling [1]. They also only require one sealed container and do not need salt pumps, transport lines, or heat tracing and operate at a wide range of temperatures depending on the PCM [3]. However, there are some disadvantages: the initial cost is higher, and PCMs have a higher risk of leaking [1].

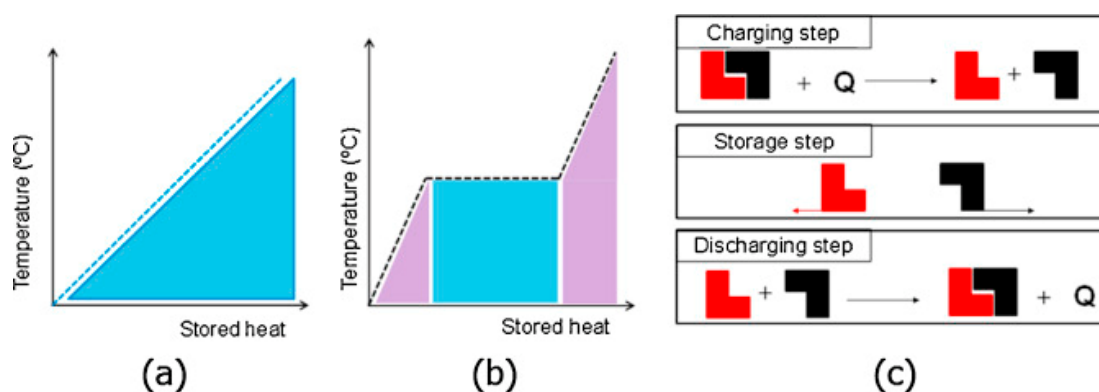


Figure 1. (a) Sensible heat, (b) latent heat, (c) thermo-chemical thermal energy storage systems (Copyright 2015 Gracia and Cabeza) [4].

1.1. Applications of LHTES Systems

LHTES systems have a wide array of applications that span across many different fields. They can aid in both heating and cooling systems, as well as energy storage, which can be converted to electrical energy. Some cooling applications include electronic cooling, air conditioning, refrigeration systems [3], lithium-ion battery cooling [5,6], and cold food packaging [6]. Some heating applications include building heating [3], waste heat recovery (for example, car exhaust, factories) [3,7] and solar food drying equipment [3].

One general energy storage application is solar power storage, which includes concentrated solar power (CSP) generation systems [7]. Even some medical applications exist, including smart textiles, which can work to either heat or cool the person depending on the need [6].

1.2. Types of PCM

PCMs can be characterized as low, middle, or high melting temperature. The potential applications of a PCM depend on its melting point, making this an important characteristic. According to Huang et al., middle temperature PCMs can be defined as those that melt between 120 and 300 °C, putting low temperature below 120 °C and high temperature above 300 °C [8]. Therefore, this paper will characterize low, middle, and high temperature PCMs according to these ranges. The following will discuss several types of PCM, all of which have a variety of melting temperatures.

1.2.1. Organic and Inorganic

Two major categories that PCMs can be split into are organic and inorganic. As shown in Figure 2, these can be further split into paraffin, non-paraffin (which include fatty acids), salt hydrates, and metallic PCMs. Paraffins are composed of straight chain n-alkanes ($\text{CH}_3-(\text{CH}_2)_n-\text{CH}_3$); the general formula for fatty acids is $\text{CH}_3(\text{CH}_2)_{2n}\bullet\text{COOH}$; salt hydrates are composed of inorganic salts and water ($\text{AB}\bullet n\text{H}_2\text{O}$), and metallic hydrates consist of metals with low melting points relative to most metals [9]. Each category has many PCMs with a wide range of phase change temperatures. Non-paraffin organic materials have the widest range of materials and properties, while paraffins are mostly commercially used. All types of PCMs have differing advantages and disadvantages due to the wide range of usable materials [9].

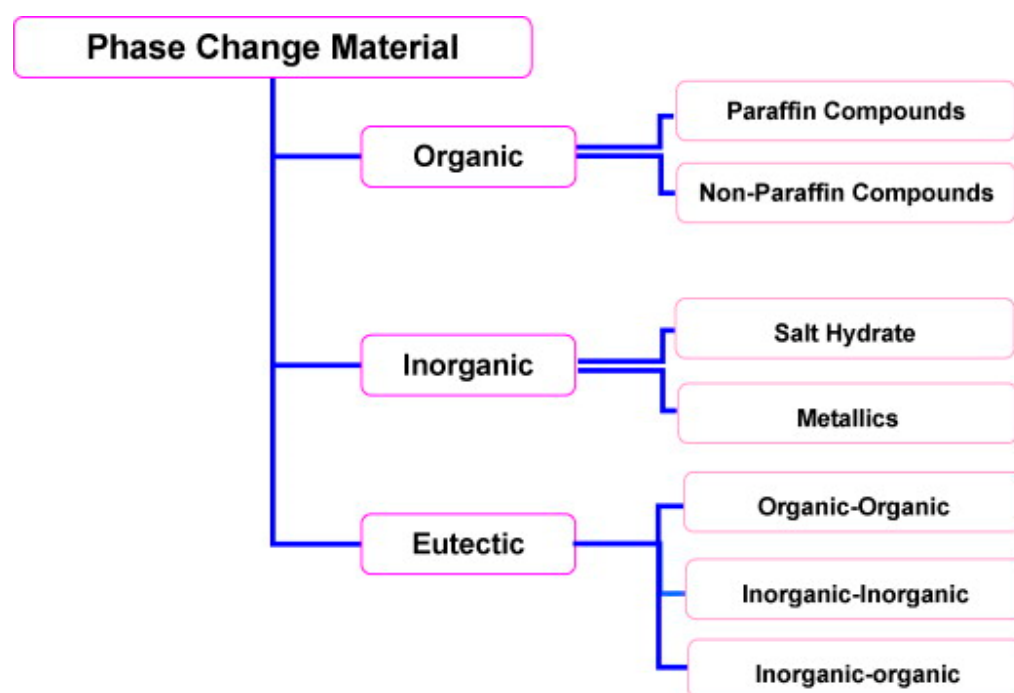


Figure 2. Major categories of PCM (Copyright 2007 Elsevier) [9].

In general, both groups of inorganic PCMs have higher thermal conductivity and latent heat of fusion per volume than organic PCMs. Salt hydrates also have a relatively small volume change, high density, and are inexpensive and readily available. However, salt hydrates can cause supercooling, phase segregation, and corrosion on metal containers. They also lack thermal stability and can be toxic. The main disadvantages of metallic PCMs include a high cost, low specific heat, and low latent heat of fusion per weight unit [1,2].

Organic PCMs have the advantages of no supercooling and high latent heat of fusion. Paraffin specifically has the advantages of being non-toxic, chemically stable, compatible with metal containers, and inexpensive. However, they have low thermal conductivity and density, have a relatively large volume change, do not have a well-defined melting point, and can be flammable. Fatty acids have a well-defined phase transition and easily reproduced phase change. They also have the disadvantage of low thermal conductivity, as well as toxicity, corrosivity, instability, and flammability, while also being much more expensive than paraffin [1,2].

1.2.2. Eutectic PCMs

Eutectic materials are another category of PCMs. A eutectic material is two or more PCMs combined in specific ratios to have the lowest possible melting point [9]. They can be a mix between multiple organic PCMs, multiple inorganic PCMs, or organic and inorganic PCMs [9]. The amount of each material can be adjusted to modify the eutectic's melting point [1]. Other advantages of eutectic materials include relatively high thermal conductivity and latent heat of fusion. A disadvantage is their high cost [2]. Raj et al. [10] used a eutectic mixture of gallium–indium metal alloy for their study. Tiari and Qui [3] used a 60:40 eutectic blend of NaNO_3 – KNO_3 . Singh et al. [11] studied eutectic LiNO_3 – KCl PCM. All of these eutectic materials proved to be effective PCMs.

2. Heat Transfer Enhancement

The main problem with PCMs is their low thermal conductivity, which makes melting and solidification times very long. A variety of passive heat transfer enhancement techniques have been developed to increase the PCM thermal conductivity and accelerate the charging and discharging process of LHTES systems and make them efficient without extra

energy input. The potential passive enhancement techniques include embedding heat pipes and fins, impregnating highly conductive porous materials with PCMs, multiple PCMs, and dispersing highly conductive nanoparticles (NPs) into PCMs. Some studies have also tested other parameters, such as orientation of the system or temperature and flow rate of heat transfer fluid (HTF). Mehta et al. [12] tested a shell-and-tube heat exchanger with stearic acid PCM in horizontal and vertical positions at different HTF temperatures. It was found that even though convection affected the rate of the first half of melting, making the horizontal position faster, the overall rate of solidification was not affected by orientation. The HTF temperature increase accelerated the melting process and increased the rate of energy stored [12]. Although these parameters can be helpful, enhancement methods have found even greater success.

Heat pipes can transport a large amount of heat over a relatively long distance to the storage media by evaporation and condensation of their working fluids. The literature has shown that they work well and can even be perfected further for optimal heat transfer enhancement. Jiang and Qu [5] used a heat pipe in a PCM-based lithium-ion battery thermal management system, where it was found that the heat pipe increased the efficiency of the cooling system significantly. Mahdavi et al. [13] developed a novel heat pipe network for LHTES application, as shown in Figure 3 [13]. Tiari et al. [14] found that an increase in HTF flow rate greatly decreased the charging time, but it had a less significant impact on the discharging time. It was also shown that increasing the HTF temperature decreased the overall charging time, while decreasing the HTF temperature decreased the overall discharging time [14].

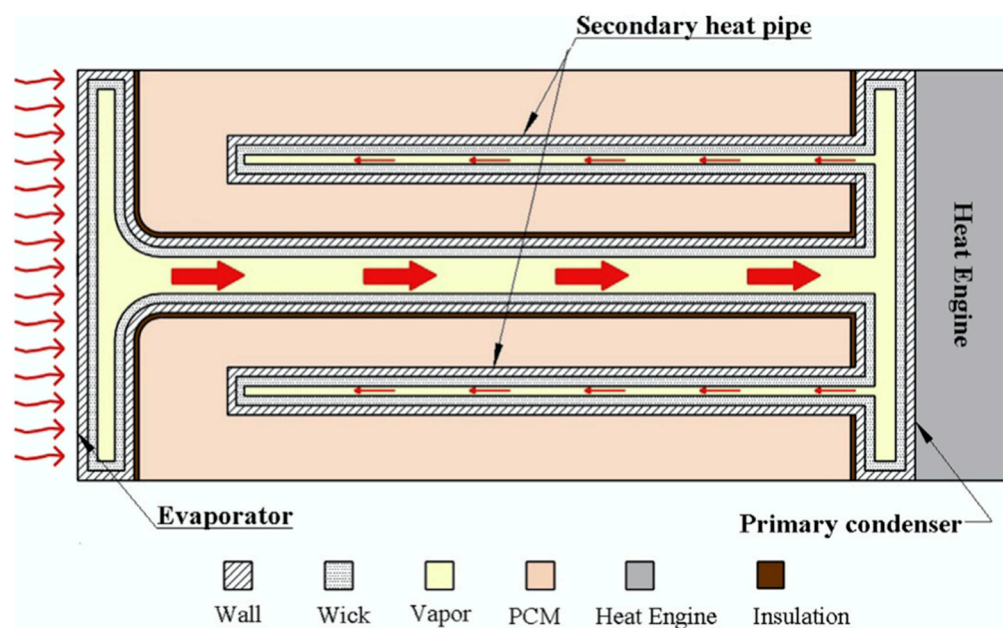


Figure 3. Heat pipe network schematic from Mahdavi et al. (Copyright 2016 Elsevier) [13].

Heat pipes are often used with the additional enhancement of fins, although fins can also be used alone. The increased contact area between the PCM and the heat transfer surfaces provided by fins enhances the PCM melting and solidification rates. Finned heat pipes have been used in several studies to improve the thermal performance of LHTES systems [3,15,16]. Tiari and Qiu found that more heat pipes resulted in better thermal performance of the LHTES system due to the lower thermal resistance between the PCM and the heat transfer surfaces [3]. Tiari et al. focused more on fins, finding that longer fins showed more uniform melting and faster charging rates after charging began; however, shorter fins had a slightly shorter total melting time. There was nearly no effect from changing the number of fins attached to the heat pipes [15]. In another numerical study,

Tiari et al. investigated the effects of fin geometry in a high-temperature LHTES system assisted by finned heat pipes, as shown in Figure 4. It was found that the length of fins did not greatly affect the overall discharging time; however, there was more uniform latent heat extraction. When increasing the number of fins, the discharging time was improved, and the container base wall temperature was increased [16]. Fins alone are also very effective, as Aly et al. [17] showed with their corrugated fins tested at different heights and numbers of corrugations. The solidification rate decreased with an increase in the corrugation height. Increasing the number of corrugations, and therefore increasing the fin length, shortened the solidification time [17]. Tiari et al. (2021) [18] also tested fins alone in the charging and discharging of a LHTES system enhanced by annular fins attached to a central pipe with HTF. For charging, twenty variable length fins with long ones on the bottom enhanced the system the most. For discharging, as well as overall for both, twenty uniform fins were the best enhancement [18]. Overall, fins were found to be an effective enhancement with and without heat pipes.

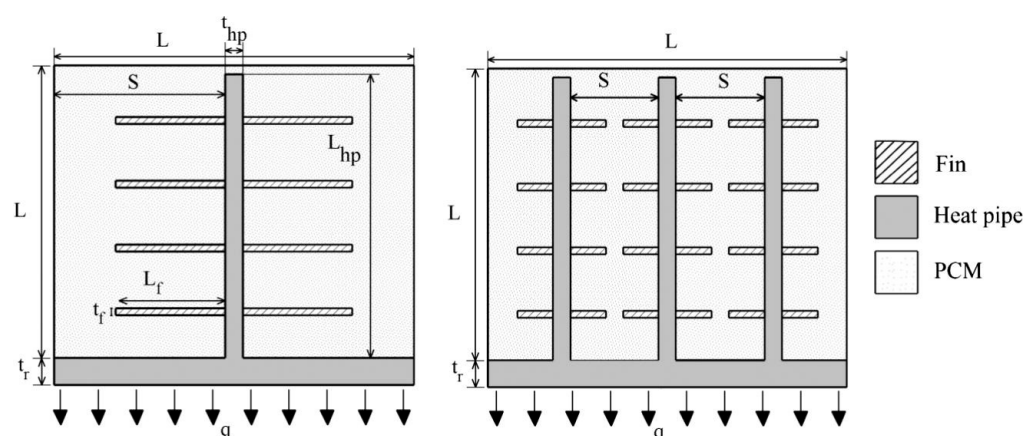


Figure 4. LHTES system assisted by finned heat pipes (Copyright 2016 Elsevier) [16].

Another effective enhancement is the impregnation of highly conductive porous materials such as metal and carbon foams as well as wools with PCMs. The PCM fills the gaps in the highly conductive material, increasing heat transfer throughout the whole system. Gasia et al. [19] studied metal wool shaped into fins and arbitrarily distributed. The systems were both an improvement over the control system, with the arbitrary distribution as the better of the two. However, during discharging, the wool showed little to no improvement over the control system [19]. Reyes et al. [20] also tested metal wool, but unlike Gasia et al., they found that it enhanced both the heating and cooling of the systems, increasing thermal conductivity and reducing the melting and solidification times [20]. Tiari and Mahdavi [21] performed a numerical study to test the melting and solidification of potassium nitrate, a high-temperature PCM, which is enhanced by copper foam and finned heat pipes. It was found that the higher foam porosity had slower melting than the lower porosity, and both showed faster melting than the pure PCM. Overall, the metal foam resulted in more uniform temperature distribution within the LHTES system [21].

A less common enhancement method is the use of multiple PCMs, which are arranged for more efficient melting and solidification. Narasimhan [22] reviewed studies that used multiple PCMs to enhance their LHTES systems. It was concluded that when multiple PCMs are placed with decreasing melting temperatures along the direction of HTF, charging times can be reduced, and if this order is reversed, discharging times can be reduced. Both cases can be achieved in one system by changing the direction of the HTF accordingly. Using multiple PCMs also can reduce the fluctuations in the exit temperature of the HTF. Of course, the total energy storage may decrease; however, as with other enhancement techniques, the payoff can outweigh this drawback [22].

Another method is nano-encapsulation, which is used to prevent the enhancement agent from interacting with the PCM, leaking, or agglomerating. Raj et al. [10] successfully prepared a layered PCM of manganese perovskite with nano-encapsulated gallium–indium eutectic metal alloy mixed in. The encapsulated particles were physically and chemically stable up to the tested 10,000 cycles. The phase transition temperature was improved by the addition of the particles, specific heat was reduced, and thermal conductivity was enhanced [10]. Li et al. [23] encapsulated octadecane PCM in polystyrene to make nano-encapsulated PCM, which they used in combination with copper foam. The nano-encapsulation allowed for shape stabilization of the PCM and prevented corrosion, leakage, and volume change during phase change. Since the particles constrained natural convection, conduction was the only source of heat transfer, and the metal foam greatly improved the system. Lower porosity foam had higher effective thermal conductivity and lower wall temperature [23].

Nano-encapsulated PCM can also be used in a slurry. Dutkowski and Kruzel [24] used Micronal DS 5039 X, an aqueous dispersion with a PMMA shell, in slurries with distilled water and a propylene glycol/water mix as base fluids. Viscosities were measured with rotational tests where torque was applied and strain was measured. The temperature range was 10–50 °C, and the encapsulated PCM content was tested in ratios from 4.3% to 43%. The viscosity increased with the increased concentration of the particles and decreased with the shear rate before reaching a plateau. The experiment successfully tested a new temperature-dependent method of finding dynamic viscosity [24]. In 2020, Dutkowski et al. [25] used the same encapsulated PCM to test changes in density during melting. The tests were conducted between 10 and 30 °C with the PCM in distilled deionized water at mass fractions between 2.15% and 8.60%. The results were compared to calculations, with matching results. The capsule did not affect the results of the PCM density. The increased concentration of the PCM in the slurry caused a decrease in the density at the same temperature range. Adding heat also decreased the density, but the density did not change proportionally [25]. Another study by Dutkowski et al. [26] was conducted with paraffin encapsulated by PMMA in a slurry with water and propylene glycol at particle mass fractions between 8.6 and 30.1 wt % to test specific heat. The samples were cooled from 50 to 10 °C. It was shown that a higher concentration of particles increased the specific heat at the melting point. The maximum specific heat varied from 9.2 at the lowest particle concentration to 33.7 kJ/kg at the highest tested concentration. The specific heat was lower at higher wt % when in liquid form but increased in solid form [26].

Finally, highly conductive NPs can be used to enhance the heat transfer to and from PCM. This method can be used alone or in combination with other enhancement methods. The idea is that evenly dispersed NPs will increase the overall thermal conductivity of the PCM without reducing the PCM volume as much as some other methods. These nano-enhanced PCM (NePCM) will be the main focus of this review. The following sections discuss studies on the effectiveness of NePCM alone, as well as in combination with the other enhancement techniques, which were described above. The NP type and shape, PCM type, additional enhancements, and other factors all affect the thermal performance of LHTES systems. Many different studies have been reviewed in this paper to paint the bigger picture of what has been done in this field and what needs to be further explored.

3. Nano-Enhanced PCM

3.1. Nanoparticles as Sole Enhancement

Elgafy and Lafdi in 2005, to the authors' best knowledge, were one of the first to study NePCMs. They experimentally and analytically studied paraffin wax enhanced with carbon nanofibers. Thermophysical properties and temperatures during solidification were recorded for different carbon nanofiber mass ratios, and the analytical model was used to predict effective thermal conductivity. The laser flash technique was used to measure thermal diffusivities. Thermal diffusivity increased with the increase in carbon fibers; however, the specific heat decreased. Increasing the carbon nanofibers decreased the

solidification time of the NePCM and increased the output power. The analytical solution was compared to the experimental results with good agreement. Modifying the nanofibers surfaces also increased the solidification rate [27].

3.1.1. Water NePCMs with Cu

Khodadadi and Hosseinzadeh were among the first researchers to study NePCMs, with their numerical model for water PCM enhanced with copper NPs. They studied the influence dispersion of NPs on the thermal conductivity, solidification rate, and latent heat of fusion. The latent heat of fusion was lowered, the rate of heat release was increased, and thermal conductivity was enhanced with the addition of NPs. It was concluded that NePCM was promising for thermal energy storage applications [28]. Jourabian and Farhadi also numerically studied the melting of ice as a PCM enhanced with copper NPs enclosed in a vertical semicircle enclosure. Different Rayleigh numbers were tested, showing that this parameter's increase strengthens buoyancy-driven convection. The NePCM was also compared to pure PCM at three Rayleigh numbers. The NPs increased the temperature of the PCM, which is an effect that increased with Rayleigh's number. NPs provided more enhancement at lower Rayleigh numbers, but there were higher melting rates at higher Rayleigh numbers. The NPs increased the thermal conductivity and decreased the latent heat of fusion. The effect of the NPs on the Nusselt number was considered to be negligible [29]. Another study using water PCM [30] numerically investigated enhancement with copper NPs. An LBM was developed and used to study how NP volume fraction and Grashof number affected heat transfer and the flow structure in NePCM. Higher Grashof numbers caused different, asymmetric convection patterns depending on the NP volume fraction. The local Nusselt number decreased with the increase in NP volume fraction, which is a result of higher thermal conductivity. Heat transfer efficiency was improved with the addition of NPs, and a higher volume fraction caused faster temperature change and melting. Energy storage was also increased with volume fraction. The copper NPs clearly enhanced the PCM melting process [30].

3.1.2. Paraffin and Alumina

Paraffin wax and paraffin-based PCMs are a popular choice, and with a wide range of low temperature melting points and compatibility with different types of NPs, they are very important to study. Akhmetov et al. [31] used COMSOL Multiphysics to numerically study two LHTES systems using two paraffin wax PCMs with low (PW-L) and high (PW-H) phase change temperatures. Al_2O_3 NPs were used to increase the heat transfer in the system. Temperature-dependent properties were used in the three-dimensional simulations. They created three mixtures for each type of wax: pure wax, 2 wt % NP, and 4 wt % NP. These mixtures were used to measure and calculate thermal and physical properties for use in the simulations. The LHTES systems were set up sequentially, with the PW-H LHTES receiving heat first and then the PW-L LHTES receiving heat. Both types of paraffin had low thermal conductivities, which were improved by the addition of the Al_2O_3 NPs. The LHTES system (shown in Figure 5) was determined to distribute energy efficiently and uniformly to the PCM containers as individual storage units. The sequential nature of the two LHTES systems was also effective [31].

As in the previous study, alumina was used in many different studies as the NP enhancement for paraffin. Abdulateef et al. [32] numerically and experimentally studied a triplex tube heat exchanger LHTES system with RT82 PCM and alumina NPs. The heat exchanger had inner and outer tubes with HTF, and a middle tube of PCM with eight equally spaced fins. The numerical study tested longitudinal and triangular fins in the same heat exchanger. The experimental results showed that the internal heating method did not fully charge the PCM, while the external heating fully melted the RT82 at a lower HTF temperature and time. The ideal HTF mass flow rate was determined to be 29.4 kg/min. The numerical study showed that the triangular fins resulted in a faster melting process, and the addition of NPs further improved the system [32].

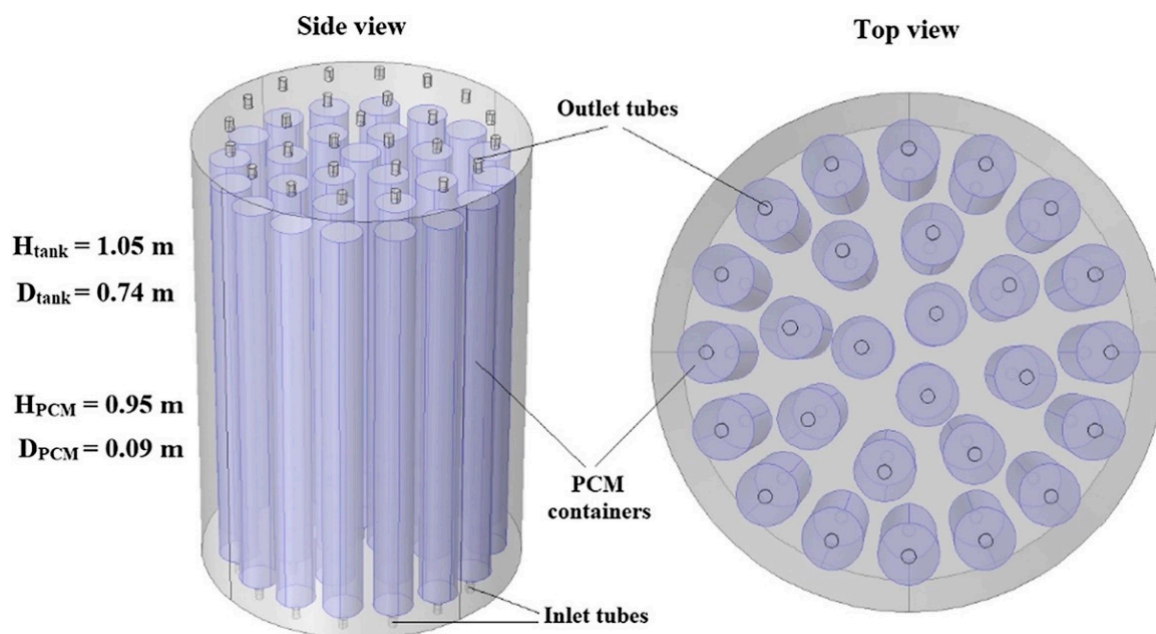


Figure 5. LHTES system configuration for the study by Akhmetov et al. (Copyright 2019 International Solar Energy Society) [31].

Zaidan and Alhamdo [33] studied a waste heat recovery system with paraffin PCM enhanced with Al_2O_3 NPs at different volume fractions both experimentally and numerically. The experimental portion used capsules of PCM, with one U tube and various volumes of NPs and a capsule with two U tubes and the ideal amount of NPs. The thermal conductivity, melting time, and solidification time were improved with the addition of NPs, with 1% being the ideal amount. Other higher amounts of NPs increased the viscosity, affecting the phase change times. The numerical simulation showed that the increased number of pipes decreased the melting time [33]. Farsani et al. [34] conducted a two-dimensional numerical study with RT 44HC paraffin and Al_2O_3 NPs in a square with a square heat source in the center and four insulated walls. The effects of heat generation rate on flow and phase change were studied; then, the effects of NPs on the melting were studied. The Rayleigh number was varied to represent the heat generation rate, and it was found that the convection vortices that formed during melting were stronger with larger Rayleigh values. Figure 6 shows the liquid fraction, average dimensionless temperature, maximum dimensionless temperature, and average Nusselt number during melting of the NePCM for a Rayleigh number of 2.72×10^6 . It was concluded that NPs had little to no influence on the Nusselt number and temperature throughout the melting process (shown in Figure 6), and therefore, they did not recommended using NPs for enhancement [34]. The conclusions of this study differ from most studies. It is possible that this is due to the parameters tested in this study, as most other studies tested the effects of the dispersion of NPs on melting time or melting percentage in a certain amount of time, or thermal conductivity.

A 2017 numerical study by Elbahjaoui and El Qarnia used paraffin enhanced with Al_2O_3 NPs in an LHTES system to investigate the effects of the aspect ratio of the PCM, volume fraction of the NPs, and the Reynolds and Rayleigh numbers on the thermal characteristics of the system. The enthalpy–porosity method was used to model melting. The study found that more NPs (higher volume fraction), a higher Rayleigh number, a higher aspect ratio, and a higher Reynolds number all decreased the melting time. Increasing the Rayleigh number also increased the SHS. A correlation was written to find the melting time, and its results matched well with the numerical results [35].

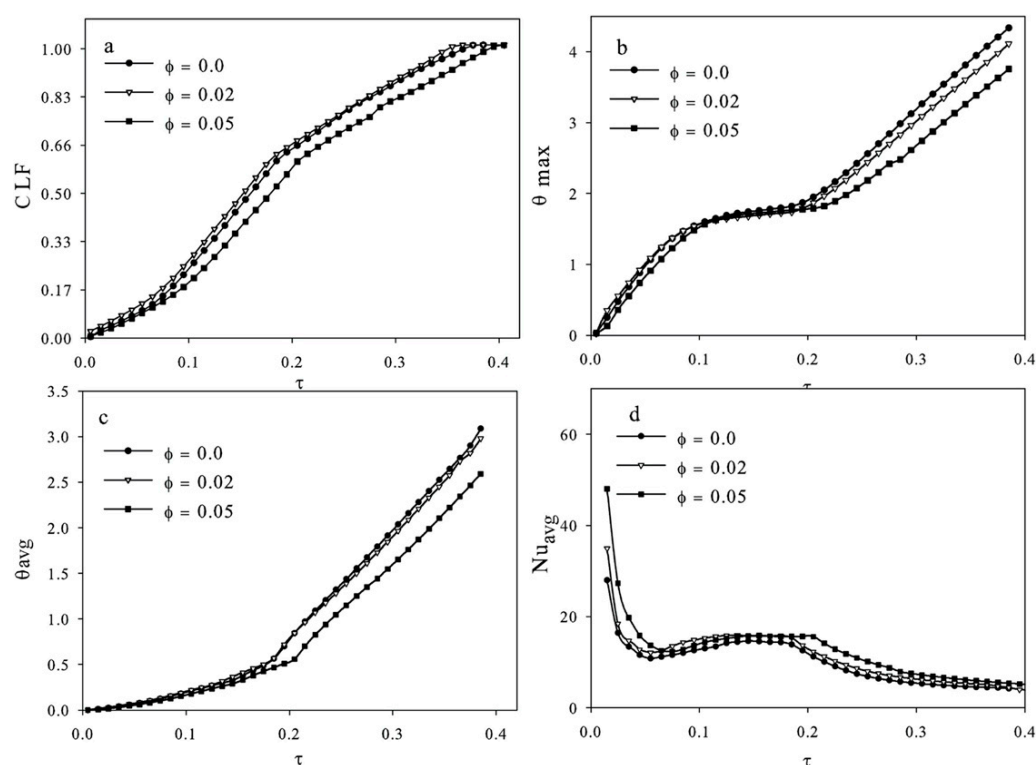


Figure 6. (a) liquid fraction, (b) average dimensionless temperature, (c) maximum dimensionless temperature, and (d) average Nusselt number in the Farsani et al. study (Copyright 2017 Elsevier) [34].

3.1.3. Paraffin and Cu

In another study by Elbahjaoui and El Qarnia, a two-dimensional numerical was developed to study the solidification of n-octadecane PCM with copper NPs, which is another popular NP type. The LHTES system consisted of rectangular slabs of PCM with HTF sandwiched in between. The enthalpy–porosity method was used to simulate the phase change process to study the effects of the NP volume fraction, PCM aspect ratio, and HTF inlet temperature on the thermal performance of the LHTES system during the discharging process. Increasing the aspect ratio and decreasing the HTF inlet temperature both improved the performance of the system. The NPs also improved the solidification rate [36].

Another use of copper NPs with paraffin is reported in a numerical study by Nie et al. They investigated two different HTF injection orientations, top and bottom, for comparison. The PCM used was paraffin RT35 with pure copper NPs, and the HTF was water. Since the previous literature was conflicting, they first found that convection plays an important role in heat transfer for top-injected HTF. Heat flux was determined to be higher in the portion (top or bottom) that the HTF was injected from. The melting time was shorter for top injection when the thickness-to-height ratio was less than 0.05; however, it was longer when the ratio was larger than this. The effect of NP was less when the ratio was increased, and NP were more effective for bottom injection than top injection. The optimum thickness-to-height ratio was determined to be 0.05 [37]. Hosseini et al. numerically investigated the melting of another paraffin-based PCM, RT 50, with copper NPs. The effect of the NP volume fraction on the melting time, liquid fraction, and penetration length were studied. A shell-and-tube model was used with water as the HTF. They found that a higher volume fraction of NPs increased the liquid fraction and the penetration length of fluid, and it decreased the melting time [38]. Algarni et al. used NePCM to improve an evacuated tube solar collector system. They experimentally studied the effects of the paraffin PCM on the performance of the system, with and without the copper NPs. The experiment

was conducted outdoors, with a pyranometer to test solar irradiation, thermocouples for temperature measurement, and a differential scanning calorimeter (DSC) to assess thermal properties. Without any PCM, the temperature of the system dropped steeply when the solar radiation decreased; however, with the addition of NePCM, the temperature decreased more gradually. The NePCM system had a 32% enhancement of efficiency overall. They minimized the agglomeration of particles with an ultrasonic vibrator. The system worked best with lower HTF mass flow rates of around 0.08 L/min. The NPs allowed for better storage on cloudy days than the non-NP storage [39]. Another study numerically modeled RT50 PCM enhanced with both Cu and Al_2O_3 NPs in a concentric tube heat exchanger. The addition of the NPs enhanced melting and heat storage, which is an effect that decreased over time for the Al_2O_3 particles. Due to an increase in the kinematic viscosity, there was a limit to the enhancement of NPs, since convection was suppressed if too many were added [40].

3.1.4. Paraffin with Carbons

Although metallic NPs are very effective, some tests with carbon-based NPs showed that they may be even more effective. Aqib et al. compared the effectiveness of paraffin enhanced with alumina (Al_2O_3) NP and nonmetallic multiwall carbon nanotubes (MWCNTs) at three different concentrations. Mixtures contained either 2, 4, or 6 wt %. The mixtures were put through charging and discharging cycles with temperatures measured by thermocouples. As the concentration of particles increased, the heat transfer increased. The MWCNTs had higher peak temperatures than alumina NPs, making them the better option for enhancement [41]. Temel and Çiftçi went a step further than just comparing types, experimentally studying the effects of NPs type, size, and shape on the thermal properties of a NePCM. They used paraffin (A82) as the PCM and tested ZnO, TiO_2 , Al_2O_3 , and MgO NPs as well as MWCNTs and graphene nanoplatelets (GNPs). They tested the particles using a scanning electron microscope (SEM) and the thermal properties using a DSC. The thermal conductivity improvements for MWCNTs, GNPs, ZnO, TiO_2 , Al_2O_3 , and MgO were 26.7, 154.9, 2.6, 3.6, 6.5, and 8.4%, respectively, when added at 5% mass fraction. The differences in enhancements were due to the thermal conductivity of the particles and shape. For tests conducted only with Al_2O_3 and MWCNTs, it was found that the increase in diameter led to an increase in thermal conductivity. NP types and mass fractions did not significantly change the melting and solidification temperatures. The melting times decreased in the same manner as the improvement in thermal conductivities, with ZnO showing the smallest improvement and the GNPs showing the greatest improvement [42].

Carbon NPs can even improve systems at incredibly small amounts. A 2018 study tested the melting and solidification of paraffin PCM with a melting range of 58–60 °C and MWCNTs. The specific heat of the NePCM was measured with DSC; then, the sample was melted and solidified, and resistance temperature detectors (RTDs) measured the temperatures. Melting times were lowest at 0.3 wt % MWCNTs, with a decrease of 30%, which was potentially due to increases in viscosity past this point. Solidification times were lowest at 0.9 wt %, with a decrease of 42.2% [43]. To test carbon NPs in a real-world scenario, Thalib et al. [44] conducted an experiment to test paraffin against graphene-enhanced paraffin in a tubular solar still (a device that desalinates water to provide potable fresh water). The experiments were conducted outdoors where the sun would provide the energy just as the device would be used. Peak temperatures of the systems throughout the day were above the 55 °C melting temperature, which were numbers that were higher with the addition of graphene into the PCM. The graphene enhanced the yield of fresh water that was produced compared to the other systems, since the heat absorbed was greater, meaning that during off hours, there was more heat stored up to release. The thermal and exergy efficiencies were also much higher with the NePCM [44].

However, not all studies found carbon NPs to be the most effective. Javadi et al. [45] studied Cu, CuO, Al_2O_3 , TiO_2 , SiO_2 , multiwall carbon nanotubes, and graphene in paraffin using a three-dimensional numerical model. The NPs were tested in different shapes and

volume fractions. Although all NPs enhanced the system, the best NP type was found to be Cu, while the worst was SiO_2 , as demonstrated by Figure 7. Then, Cu was tested at different volume fractions, and 0.2 was the ideal volume fraction to increase the thermal conductivity up to 55%. Cu was also tested in different shapes, and the “blade” shape (a long, thin, 3D ellipse-like shape) was the most efficient shape for enhancement when compared with spherical, brick, cylindrical, and platelet-shaped NPs [45].

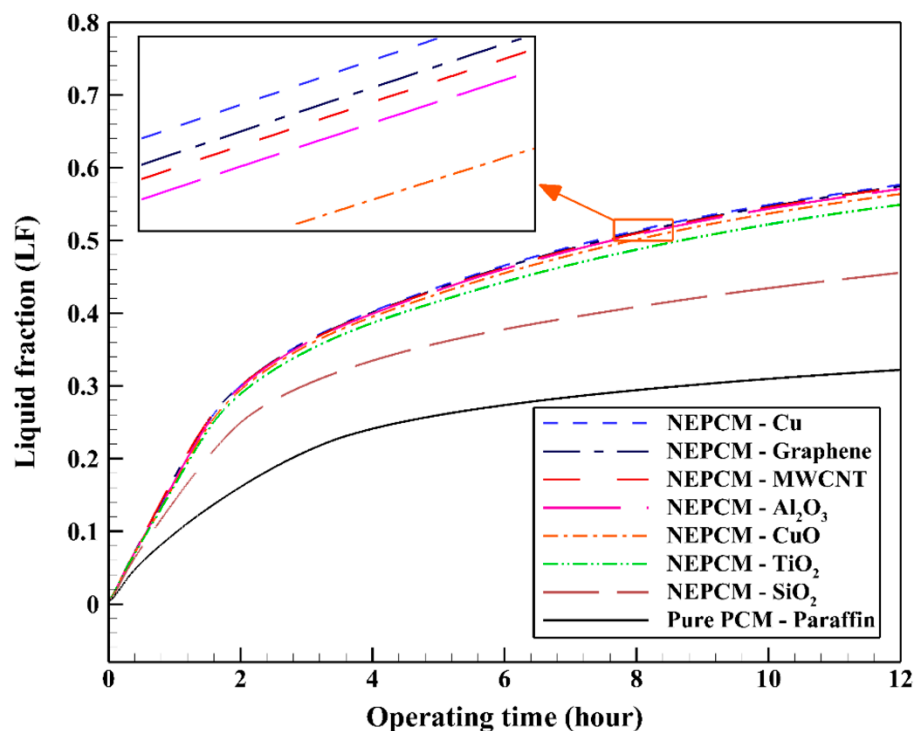


Figure 7. Liquid fractions of the different NePCMs tested over time by Javadi et al. (Copyright 2020 Javadi et al. <https://creativecommons.org/licenses/by/4.0/>) accessed on 18 June 2021 [45].

Similar to Javadi et al. [45], Bashar and Siddiqui [46] found MWCNTs to be less effective. Four different types of NPs were compared in an experimental study. Paraffin was used as the PCM with silver, copper oxide, aluminum oxide, and MWCNTs. The PCM was heated, and thermocouples were used for temperature measurements. All of the NPs enhanced the heat transfer; however, silver was the most effective, which was followed by copper oxide. Aluminum oxide and the MWCNT were much less effective because they sunk to the bottom of the PCM. Then, copper oxide was tested in varying mass fractions, 1, 3, 6, 8, and 10%, and it was found that the 6% mass fraction performed best [46].

3.1.5. Paraffin with Other NPs

A variety of metal oxide NPs were used to enhance RT82 PCM by Khatibi et al. [47] using a numerical study, including some of the ones above. Al_2O_3 , ZnO, CuO, and SiO_2 were added to the PCM to study the solidification process and test different HTF temperatures and tube diameters in three different LHTES units. The systems were a triplex-tube and two shell-and-tube, one with inner cooling and the other with outer cooling. The triplex tube system was modeled for all of the NP comparison studies; then, the different systems were compared, with and without NPs. All of the NPs reduced the solidification time, with Al_2O_3 having the largest impact, which was followed by ZnO, CuO, and SiO_2 in decreasing order, for a volume fraction of 0.02. For a volume fraction of 0.04, CuO had the greatest impact, which was followed by ZnO, Al_2O_3 , and SiO_2 , in that order. The decrease in solidification time was caused by the increase in thermal conductivity and decrease in the latent heat of fusion. The triplex-tube system had the best performance, and external

cooling the second best. The effect of the NPs was diminished with a decrease in HTF temperature and was also affected by the type of LHTES system [47].

Even though SiO_2 NPs were found to be the least effective of those above, they can still be an effective enhancement. It may be that they work best at lower temperatures such as in the following system. Dastmalchi and Boyaghchi [48] used a numerical model to study a PCM–air heat exchanger with respect to exergy and cost per unit exergy for peak and off peak. The system worked along with an air conditioning system, using cool outdoor or indoor air to solidify PCM during off-peak times, and using the PCM to help cool the hot indoor air during peak times. The two-dimensional model was used to numerically perform an energy analysis, exergy analysis, and an exergoeconomic analysis. They simulated the temperatures of a typical week in late June in Esfahan, Iran. The PCM used was RT25 enhanced with SiO_2 particles. Cooling power increased for low night temperatures and high day temperatures. Exergy efficiency was low during peak hours at higher indoor temperature setpoints. Setpoint ranges from 23 to 26 °C had the lowest cost and those from 24 to 25 °C had the highest cost with respect to exergy. The cost increased with increased slab length and with increased airflow due to the fan and compressor. Exergy efficiency increased at peak time and exergy destruction increased at off-peak time when NPs were added [48]. Pasupathi et al. [49] also found success with SiO_2 when combined with CeO_2 . They experimentally assessed the properties of paraffin PCM with hybrid $\text{SiO}_2/\text{CeO}_2$ NPs at different mass percentages. At 2%, the particles begin to agglomerate, but they were evenly distributed up to that point. The NPs reduced the difference between the melting and solidification temperatures of the paraffin and delayed thermal decomposition. The thermal conductivity improved greatly up to 1% NPs and minimally above that percentage, as can be seen in Figure 8. It was concluded that 1% NPs was the best amount for enhancement [49].

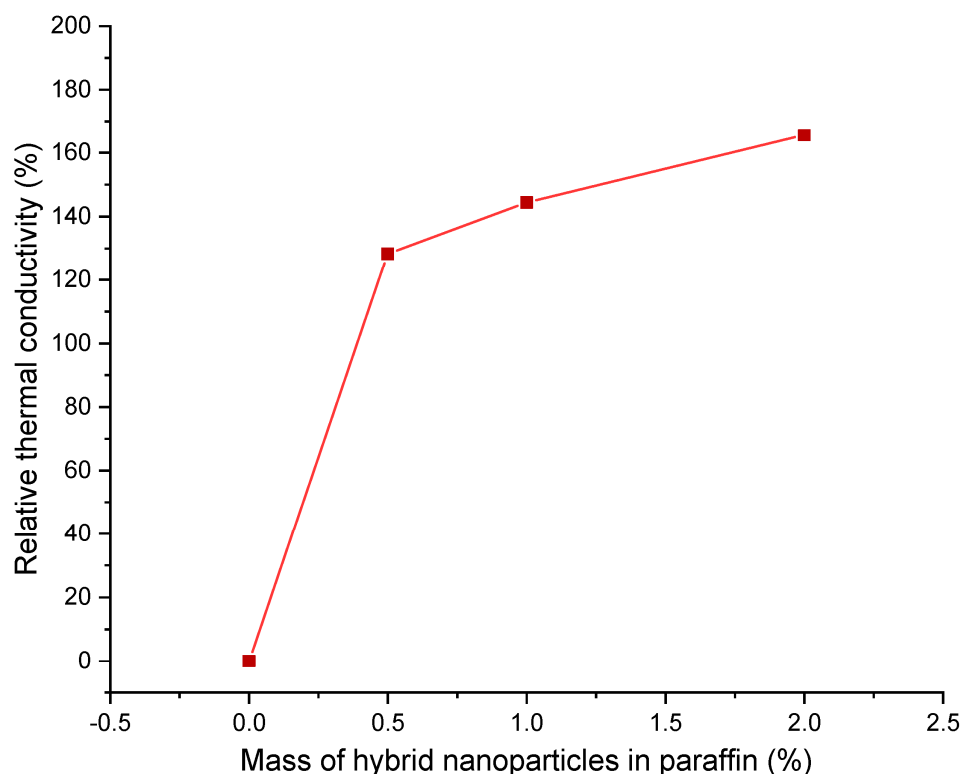


Figure 8. The relative enhancement in thermal conductivity with the addition of NPs (Copyright 2020 Pasupathi et al. <https://creativecommons.org/licenses/by/4.0/legalcode>) accessed on 18 June 2021 [49].

Another type of commonly used NP is plain aluminum. A study conducted by Zhou et al. [50] numerically and experimentally analyzed octadecane paraffin enhanced with aluminum NPs. Three-dimensional octadecane molecule models were created and made into a cubic unit cell, and aluminum was added into the unit cell. The non-equilibrium molecular dynamics method was used for the thermal conductivity simulation. The simulation showed that thermal conductivity increased with an increasing percentage of NPs; however, it increased more in the liquid PCM than the solid PCM. The experimental portion of the study used the transient thermal probe method to find thermal conductivity at room temperature (290 K) and at 320 K when the PCM is melted. The results showed that thermal conductivity increased with increase in aluminum particles. Comparing the two, the thermal conductivities followed the same trend, although the simulation values were smaller [50].

An interesting NP type was designed by Badakhsh et al. [51], who experimented with the melting and solidification of paraffin with aluminum nitride coated SiC (SiC@AlN) particles. SEM, laser diffraction, XRD, and DSC were used for characterization, among other methods. The effects of milling frequencies and the ball-to-powder mass ratio on the particle size distribution were tested: as the frequency increased, the particle diameter decreased. Thermal conductivity and specific heat testing by the transient plane source method showed that the SiC@AlN particles achieved higher thermal conductivity and lower specific heat than the other cases (plain paraffin, paraffin with AlN, paraffin with SiC). X-ray spectrometry showed that this was caused by the formation of conductive networks by the SiC@AlN particles. An insignificant growth in latent heat was also observed, and the SiC@AlN particles were less expensive than AlN alone [51]. Another study with SiC particles also found them to be a promising enhancement. Maher et al. [52] compared two different nanomaterials in paraffin wax to improve thermal conductivity. After synthesis of the nanocomposites, they were characterized by a field emission SEM (Shown in Figure 9) as well as a DSC and laser flash apparatus, which was used to find thermal conductivity. The SiC-enhanced PCM had better thermal conductivity than the Ag-enhanced PCM, with the largest amount, 15 wt %, showing the best results. However, latent heat, melting temperature, and specific heat capacity were reduced by the NPs. This means that the highest weight percent is not always ideal, and the amount of NPs should be optimized on a case-by-case basis [52].

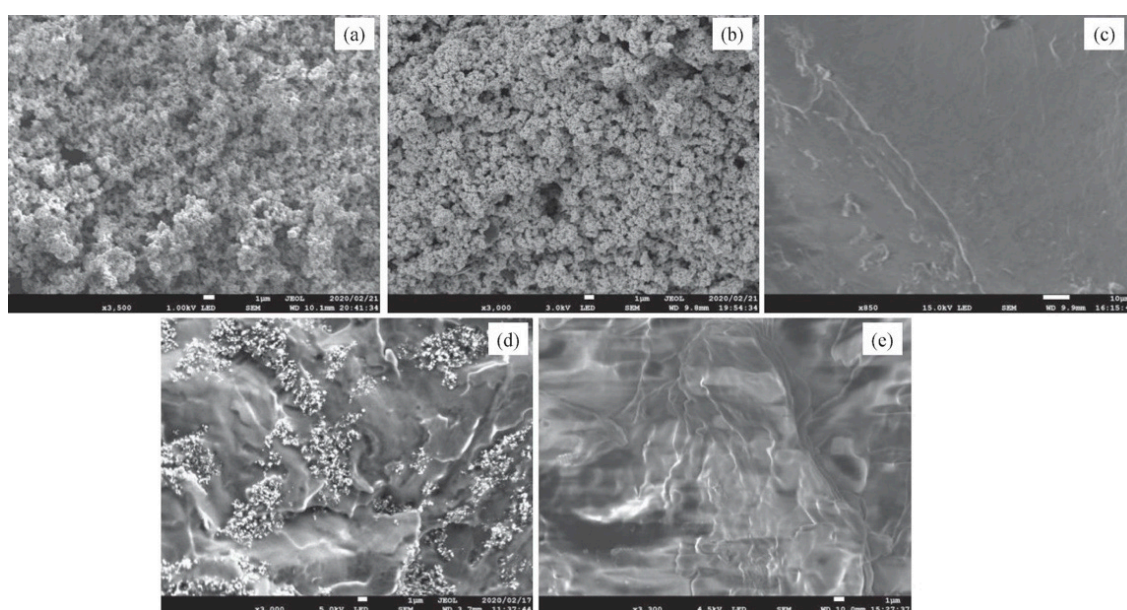


Figure 9. SEM images of (a) Silicon carbide, (b) Silver, (c) Pure paraffin wax, (d) Paraffin–SiC composite, and (e) Paraffin–Ag composite from Maher et al. (Copyright 2020 Elsevier) [52].

Ghalambaz et al. [53] numerically studied unspecified 2D hybrid NPs dispersed in a square of octadecane paraffin PCM. A “linearized correlation procedure” was used to find the properties of hybrid nanofluid to use in the simulations. They varied NP volume fraction, conductivity, and viscosity to test their effects. It was found that a large thermal conductivity and small viscosity resulted in shorter melting times. Initially, the mushy zone was thicker at the solid–liquid interface due to the lower convection there; however, over time, this phenomenon went away. A case study was also done with water and Ag-MgO NPs, which showed that these hybrid particles were more effective than plain MgO particles [53].

3.1.6. Eutectic Hydrate Salts

Other types of low-temperature PCMs are less commonly used; however, they can still have many benefits over water or paraffin. Liang and Chen [54] experimentally studied the solidification of eutectic hydrate salts with carbon NPs. Three samples with different amounts of thickeners were tested, showing an increase in onset and end temperatures from 0 to 3 wt %, but a decrease at 5 wt %. With increasing viscosity, the effects of the NPs lessened, as did the absorption peak and phase change enthalpy, due to the decrease in micro-convection. Melting latent heat was decreased compared with ice and decreased with increased viscosity. The increase in viscosity also suppressed supercooling, decreased surface tension, and decreased the solidification time. Nucleating agents were proven to reduce or eliminate the degree of supercooling. Stability testing showed that after 20, 30, and 50 cycles, the supercooling reduced [54]. The salt hydrate Th29 was studied numerically by Jamalbadi et al. [55] as a heat sink for electronic circuits. The NePCM, which was enhanced with Cu NPs, was in a rectangular container next to a surface acoustic wave system. Three volume fractions were tested, and an increase in NP increased heat transfer at the solid–liquid interface. The NePCM improved the heat transfer by up to 10% [55].

3.1.7. PEG and Ag

Marcos et al. [56] characterized polyvinylpyrrolidone-treated silver NPs in polyethylene glycol (PEG) PCM for low temperature applications. The NPs were added at mass percentages from 0.10 to 1.1%. They analyzed the dynamic viscosity, isobaric heat capacity, density, and surface tension of the samples as well as the thermal conductivity and diffusivity. Properties were analyzed using UV-Vis spectroscopy, scanning transmission electron microscopy, mass spectrometry, TGA, dynamic light scattering, and DSC. Thermal conductivity was improved up to 3.9% by the 1.1 wt % NPs. Undesirable sub-cooling was also reduced with the addition of NPs [56]. Song et al. [57] created silver–halloysite nanostructures with silver NPs on 1D halloysite nanotubes to disperse in PEG PCM, which is a surfactant–fatty acid. The goal was to create a “form-stable” PCM that could be used without additional encapsulation, was form stable during phase change, inexpensive, and easily molded into different shapes. The silver particles were added to improve thermal conductivity, and the halloysite was used as a supporting material. The thermal conductivity in the nanocomposite was greatly improved from pure PEG [57]. A study by Qian et al. [58] also experimentally researched PEG but combined with diatomite and enhanced with Ag. SEM, TEM, Energy-Dispersive X-ray Spectroscopies, XRD, DSC, and TGA were used to characterize the sample. The Ag NPs were evenly distributed, and the material had good chemical compatibility and thermal stability, with improvements in supercooling. The thermal conductivity was improved by 127% with the addition of NPs and melting and freezing times were reduced [58].

3.1.8. Fatty Acids

Another group of PCMs that can be low temperature is fatty acids. Prabakaran et al. [59] experimentally investigated the solidification of the fatty acid PCM OM08 with graphene NPs. The setup was a sphere of aluminum filled with PCM and strategically placed

temperature sensors in a constant cool temperature bath. The PCM was melted and brought up to 31 °C; then, it was immersed in the −10 °C cooling bath. This was conducted for the PCM with and without the NPs. The thermal conductivity increased greatly with increasing NP volume percentage (102% maximum), with a sharp increase when solidification occurred. The addition of NPs caused the fluid to have non-Newtonian behavior. The solidification time was also shorter with the increase in NPs, up to a 39% reduction [59].

Santhosh et al. [60] used a fatty acid called myristic acid with Fe₂O₃ NPs at several different concentrations to test whether the particles enhanced the performance of the LHTES system. This experimental study examined both melting and solidification by monitoring the temperature every 30 s during both processes. Melting and cooling rates increased with the concentration of NPs, due to increased thermal conductivity [60]. Barreneche et al. [61] characterized two more fatty acid NePCMs: palmitic acid and capric acid PCMs enhanced by CuO NPs. SEM, X-ray diffraction, Fourier-transform infrared spectroscopy (FTIR), and thermogravimetric analysis (TGA) were used to characterize the NePCMs. The samples were melted, and thermal conductivity and latent heat storage were tested. Thermal conductivity increased until 1.5 wt % NPs for the capric acid and up to 3.0 wt % for palmitic acid. Maximum heat storage was achieved at 1.0 wt % for both [61].

3.1.9. Various Middle Temperature PCMs

A common middle-temperature PCM is erythritol, which is a sugar-alcohol. Mayilvelnathan and Valan Arasu [62] performed an experimental study on the dispersed graphene NPs in erythritol PCM in three different concentrations. The NPs distributed randomly in all samples and did not chemically interact with the PCM during 100 melting/solidifying cycles. An increase in NP concentration increased the latent heat of fusion, decreased the melting temperature, decreased the latent heat of solidification, and increased the solidification temperature. Thermal conductivity also increased with the increase in NP [62]. Another experimental study by the same authors was conducted with erythritol PCM and graphene NPs [63]. DSC was used to find the latent heat of fusion and the melting temperature of the PCM with and without the NPs, and the laser flash method was used to find thermal conductivities. The NPs decreased the melting temperature and increased the solidification temperature while reducing sub-cooling of the erythritol. Hot oil was the HTF in the helical tube, which was used at different flow rates and inlet temperatures. Increasing the HTF inlet temperature for melting and decreasing for solidification enhanced heat transfer, decreasing the onset time. This enhancement was even better in the NePCM. The increased HTF flow rate sped up melting and solidification, with a more significant difference in melting time. The NPs reduced the melting and solidification times, melting temperature, and latent heat of melting. They also increased the thermal conductivity and decreased subcooling. They concluded that the system was an effective energy storage system [63]. Manickam et al. [64] also experimented with erythritol PCM, which was enhanced with TiO₂ and CNT NPs. The NePCM was cycled through melting and solidification on a hotplate while thermocouples measured temperatures. They recorded the melting temperature, melting time, and solidification time for 25 cycles. DSC and TGA were used to further characterize the PCM. The phase change temperature was between 118 and 124 °C, with the addition of NPs responsible for the higher temperatures. Latent heat increased, as did chemical and thermal stability. Melting and solidification times were reported as around 12 min, but times were not compared between cases. It was concluded that this material would be good for solar thermal applications [64].

Another middle-temperature PCM is D-mannitol, which is a sugar alcohol. Mekrisuh et al. [65] numerically simulated the melting of this PCM with a few enhancement methods. Although the system was enhanced with fins and GNPs, the optimization of geometry was the main purpose of this study. It was found that adjusting the outer diameter and height of the LHTES system while keeping the diameter of the heat transfer tube constant is the best method for optimizing the geometry. The enhancement techniques

were added to prove that the geometry optimization had greater effects than any other enhancements would. Even with both fins and nano-plates, the time to melt was twice that of optimizing the geometry [65].

An interesting middle-temperature eutectic, $\text{LiNO}_3\text{-KCL}$ PCM, studied by Singh et al. [11] was enhanced with different concentrations of COOH-functionalized graphene nano-platelets (f-GNP). The thermophysical properties of the nano-composite were found with DSC, and thermal conductivities were studied with laser flash analysis. The f-GNP accelerated the melting and solidification processes, at 5%. At 1%, the f-GNP actually increased the melting time due to the increase in viscosity. This is due to the enhancement of thermal conductivity with the addition of the GNPs. The specific heat also increased with greater concentration of f-GNPs, and the latent heat was reduced [11].

3.1.10. $\text{NaNO}_3\text{-KNO}_3$

The $\text{NaNO}_3\text{-KNO}_3$ mixture is one of the more common middle-temperature PCMs used with NPs. Chieruzzi et al. [66] experimented with the melting and solidification of an $\text{NaNO}_3\text{-KNO}_3$ mixture PCM enhanced with SiO_2 , Al_2O_3 , TiO_2 , and $\text{SiO}_2\text{-Al}_2\text{O}_3$ NPs. The NPs were added in three weight fractions; then, DSC and SEM were used for characterization. All of the NPs reduced the onset and melting temperatures of the PCM. The NPs also increased the specific heat and heat of fusion. The 1.0 wt % concentration was the most effective by far, as were the $\text{SiO}_2\text{-Al}_2\text{O}_3$ NPs, although the other types of NPs were also effective [66]. Another study by the same authors [67] also used $\text{NaNO}_3\text{-KNO}_3$ PCM enhanced with SiO_2 , Al_2O_3 , and a $\text{SiO}_2/\text{Al}_2\text{O}_3$ mixture of NPs at 1.0 wt %. These were tested at different processing screw speeds (100/200 rpm) and mixing times (15/30 min). An SEM was used to evaluate the dispersion of the NPs in the samples. The study found that the thermal properties of the samples depended on the processing and the NP type. The most effective were the silica/alumina NPs that were mixed for 30 min at 200 rpm. They had the highest specific heat and stored heat along with the lowest onset temperature [67]. Aslfattahi et al. [68] also used $\text{NaNO}_3\text{-KNO}_3$ PCM, but with MgO NPs. SEM was used to check the dispersion of NP, and DSC was used to measure the enthalpy and melting point. Both the enthalpy and melting point decreased with the addition of NPs. This indicated better thermal conductivity at the melting point. TGA was also used to assess thermal stability and mass loss, which showed that the thermal stability was enhanced at high temperatures [68]. A study by Saranprabhu and Rajan [69] also tested the combination $\text{NaNO}_3\text{-KNO}_3$ solar salt with MgO NPs for solidification and thermal properties. Thermal conductivity increased with MgO NPs concentration up to 0.25 wt %. Thermal diffusivity also increased with the addition of NPs, while latent heat did not change below 0.125 wt %, and it was reduced slightly at higher concentrations. Solidification time was reduced with the addition of MgO, as was the discharge rate, and again, both were best at 0.25 wt %. Due to these results, 0.25 wt % was deemed the most effective concentration [69].

Myers et al. [70] experimentally investigated a eutectic mixture of $\text{KNO}_3\text{-NaNO}_3$ (a middle-temperature PCM) along with KNO_3 and NaNO_3 PCMs (high temperature) enhanced with 2% volume CuO NPs. The melting temperatures were around 306, 334, and 220 °C for the sodium nitrate, potassium nitrate, and eutectic mixture, respectively and these melting temperatures did not change significantly with the addition of the CuO NPs. Thermal diffusivity improved in all cases, especially with the eutectic mixture. The materials also held up under thermal cycling without degradation. Higher NP concentrations were tested next, but it was found that these produced a lot of uncertainty in measurements, which is probably due to agglomeration at high concentrations [70].

3.1.11. High-Temperature PCMs

Another study by Chieruzzi et al. [71] focused on a high temperature PCM, experimentally testing KNO_3 PCM with 1 wt % silica (SiO_2), alumina (Al_2O_3), and $\text{SiO}_2\text{-Al}_2\text{O}_3$ NPs. The goal was to develop a PCM with a melting point between 300 and 350 °C with

these materials. In solid phase, NPs increased the specific heat by about 5–10% and in liquid phase around 6%. Of the different NPs, the silica was the most promising, lowering the phase change temperature of the KNO_3 by 3 °C and increasing the latent heat of fusion up to 12%. SEM showed that the silica particles were dispersed more uniformly than the other NPs. It was concluded that the materials would be useful for concentrated solar power (CSP) systems [71].

A different high-temperature PCM also for CSP application was designed by Xiong et al. [72], who created a eutectic mixture of sodium bromide, potassium bromide, lithium bromide, and calcium bromide enhanced with SiO_2 NPs. Three different diameters and different concentrations of SiO_2 were tested, at different wt % between 0.1 and 2.0 wt %, with 22 samples total. Melting points were analyzed using a simultaneous thermal analyzer, while the samples were raised from 30 to 900 °C. The bromides had individual melting points above 700 °C (with the exception of LiBr at 550 °C); however, the eutectic mixture had a melting point of 313 °C, which varied only a little (310–314 °C) with the addition of NPs. Generally, the addition of NP decreased the melting temperature, apart from 10 nm particles at 2.0 wt % concentration. The heat of fusion increased with NP concentration, reaching a maximum before decreasing with higher concentrations. This occurred for all diameters, with larger diameters yielding smaller numbers. The heat of fusion increased drastically with increase in wt %. However, it showed varying reactions to increased diameter depending on the wt % added. Decomposition points all decreased drastically up to 22 nm diameter and then increased from that point [72]. Similarly, Han et al. [73] experimented with another mixture of high melting temperature PCM— $\text{KCl}:\text{MgCl}_2:\text{NaCl}$ enhanced with Al_2O_3 , CuO , and ZnO NPs. Latent heat decreased slightly with the addition of NPs, but sensible heat increased, causing little overall change in thermal energy storage capacity. Thermal diffusivity and thermal conductivity were increased, with the greatest enhancement being Al_2O_3 particles, which was followed by CuO and ZnO . TGA showed excellent thermal stability, again with Al_2O_3 showing the biggest enhancement. It was concluded that the best NP for enhancement of this PCM was Al_2O_3 [73].

A variety of PCMs and NPs have been studied, with a large amount of paraffin-based PCMs, in a combination of numerical and experimental studies. In nearly every case, NPs were found to be an effective enhancement to the PCM. When NP types were compared, the most effective NP varied by study and the types compared. It seems to depend on the PCM used and the melting temperature. Future work could potentially include trying different melting temperatures with different NP types to develop a correlation. The “best” NP is very situational, depending on the application of the NePCM, base PCM, and the PCM melting temperature. Table 1 summarizes the studies reviewed in this section.

Table 1. A summary of studies that only used NPs to enhance the PCM thermal properties.

Authors	PCM Melting Point (°C)	Nanoparticle Type	Phase Change Process	Study Case	Result
Elgafy and Lafdi (2005) [27]	Paraffin wax (67 °C) Low	Carbon nanofibers	Solidification	Experimental and analytical (1D)	The nanofibers enhanced the PCM performance
Khodadadi and Hosseinzadeh (2007) [28]	Water (0 °C) Low	Cu	Solidification	Numerical	The NPs enhanced the heat transfer and solidification
Jourabian and Farhadi (2015) [29]	Ice (0 °C) Low	Cu	Melting	Numerical (2D)	NPs increased the thermal conductivity
Feng et al. (2015) [30]	Water (0 °C) Low	Cu	Melting	Numerical (2D)	The Cu NPs enhanced the system

Table 1. Cont.

Authors	PCM Melting Point (°C)	Nanoparticle Type	Phase Change Process	Study Case	Result
Akhmetov et al. (2019) [31]	Paraffin wax (PW-L: 44–48 °C PW-H: 64–66 °C) Low	Al ₂ O ₃	Melting and solidification	Numerical (3D)	Both paraffin thermal conductivities were improved by the NP
Abdulateef et al. (2021) [32]	Paraffin RT82 (78.15–82.15 °C) Low	Al ₂ O ₃	Melting	Experimental and numerical (2D)	The addition of NPs improved the system
Zaidan and Alhamdo (2018) [33]	Paraffin (63 °C) Low	Al ₂ O ₃	Melting and solidification	Experimental and numerical (3D)	1% was the ideal amount of NPs
Farsani et al. (2017) [34]	Paraffin (RT 44HC) (45 °C) Low	Al ₂ O ₃	Melting	Numerical (2D)	Little to no improvement from NPs
Elbahjaoui and El Qarnia (2017) [35]	Paraffin wax (47 °C) Low	Al ₂ O ₃	Melting	Numerical (2D)	Increased NP, Reynolds number, Rayleigh number, and aspect ratio all decreased melting time
Elbahjaoui and El Qarnia (2017) [36]	n-Octadecane (28.2 °C) Low	Cu	Solidification	Numerical (2D)	NP, increased aspect ratio, and decreased HTF inlet temperature all improved performance
Nie et al. (2021) [37]	Paraffin RT35 (29–36 °C) Low	Cu	Melting	Numerical (2D)	Melting time shorter for top injection when $R < 0.05$, but longer with larger R. NP more effective for bottom injection
Hosseini et al. (2013) [38]	RT 50 (48 °C) Low	Cu	Melting	Numerical (3D)	Increased NP enhanced the system
Algarni et al. (2020) [39]	Paraffin wax (52 °C) Low	Cu	Melting and solidification	Experimental	NePCM enhanced efficiency by 32%
Nitsas and Koronaki (2020) [40]	RT50 (45–51 °C) Low	Cu and Al ₂ O ₃	Melting	Numerical (2D)	NPs enhanced melting
Aqib et al. (2020) [41]	Paraffin wax (55–58 °C) Low	Al ₂ O ₃ and nonmetallic NPs, multiwall carbon nanotubes	Melting and solidification	Experimental	MWCNT worked better than Al ₂ O ₃
Temel and Çiftçi (2018) [42]	Paraffin wax (82 °C) Low	Al ₂ O ₃ , TiO ₂ , MgO, ZnO, MWCNTs and Graphene nanoplatelet	Melting and solidification	Experimental	GNPs showed the best improvement
Murugan et al. (2018) [43]	Paraffin (18–23 °C) Low	MWCNT	Melting and solidification	Experimental	Melting improved up to 0.3 wt % MWCNT, solidification up to 0.9 wt %
Thalib et al. (2020) [44]	Paraffin (55 °C) Low	Graphene	Melting and solidification	Experimental	Graphene NPs greatly enhanced the system

Table 1. Cont.

Authors	PCM Melting Point (°C)	Nanoparticle Type	Phase Change Process	Study Case	Result
Javadi et al. (2020) [45]	Paraffin (n-Octadecane) (28 °C) Low	Cu, CuO, Al ₂ O ₃ , TiO ₂ , SiO ₂ , multi-wall carbon nanotube, and graphene	Melting	Numerical (3D)	Cu at 0.2 concentration in blade shape were the best
Bashar and Siddiqui (2018) [46]	Paraffin wax, Polyfin (55 °C) Low	Silver, copper oxide, aluminum oxide, MWCNTs	Melting	Experimental	Silver and copper oxide performed best
Khatibi et al. (2021) [47]	RT82 (76.9–84.9 °C) Low	Al ₂ O ₃ , CuO, SiO ₂ , ZnO	Solidification	Numerical (2D)	CuO at 0.04 volume fraction were ideal
Dastmalchi and Boyaghch (2020) [48]	RT25 (23–25 °C) Low	SiO ₂	Melting and solidification	Numerical (2D)	Used properly, the system decreased the cost of the AC
Pasupathi (2020) [49]	Paraffin (63.74 °C) Low	SiO ₂ , CeO ₂	Melting	Experimental	1% NP showed best improvement
Zhou et al. (2016) [50]	Octadecane Paraffin (27–29 °C) Low	Aluminum	Melting	Numerical (3D) and experimental	Thermal conductivities improved with Al %
Badakhsh et al. (2018) [51]	Paraffin (53–57 °C) Low	AlN-coated SiC	Melting and solidification	Experimental	The particles were successful at enhancing the system
Maher et al. (2021) [52]	Paraffin wax (≈52 °C) Low	SiC and Ag	Melting	Experimental	SiC enhanced at 15 wt % showed best results
Ghalambaz et al. (2017) [53]	Octadecane Paraffin (30 °C) Low	Hybrid NPs	Melting	Numerical (2D)	Large conductivity and low viscosity worked best, hybrid particles worked better than non-hybrids
Liang and Chen (2018) [54]	Eutectic hydrate salts (−11.9, −10.6, and −14.8 °C) Low	Carbon	Solidification	Experimental	A good balance for viscosity can increase efficiency of NePCM
Jamalabadi (2021) [55]	Th-29 (Mostly CaCl ₂ ·H ₂ O) (29 °C) Low	Cu	Melting	Numerical (2D)	NPs improved the system
Marcos et al. (2020) [56]	Polyethylene glycol (4 °C) Low	Ag	Melting and solidification	Experimental	Thermal conductivity was improved up to the highest tested percent (1.1 wt %)
Song et al. (2019) [57]	Polyethylene glycol (33.6 °C) Low	silver on 1D halloysite nanotube	Melting and solidification	Experimental	Nanostructures improved thermal conductivity
Qian et al. (2012) [58]	Polyethylene glycol/diatomite (60.51 °C) Low	Ag	Melting and solidification	Experimental	The Ag enhanced the PCM
Prabakaran et al. (2019) [59]	OM08 (8–9 °C) Low	Graphene	Solidification	Experimental	The graphene sped up solidification and improved thermal conductivity

Table 1. Cont.

Authors	PCM Melting Point (°C)	Nanoparticle Type	Phase Change Process	Study Case	Result
Santhosh et al. (2020) [60]	Myristic acid (54.4 °C) Low	Fe ₂ O ₃	Melting and solidification	Experimental	NP increased melting and solidification times
Barreneche et al. (2019) [61]	Capric acid (32 °C) Palmitic acid (64 °C) Low	CuO	Melting	Experimental	CA was enhanced up to 1.5 wt % NPs, PA up to 3.0 wt %
Mayilvelnathan and Arasu (2019) [62]	Erythritol (120 °C) Middle	Graphene	Melting and solidification	Experimental	Increased NP increases thermal conductivity
Mayilvelnathan and Arasu (2020) [63]	Erythritol (120 °C) Middle	Graphene	Melting and solidification	Experimental	The NPs enhanced the system
Manickam et al. (2019) [64]	Erythritol (120 °C) Middle	TiO ₂ and CNTs	Melting and solidification	Experimental	This material would be good for solar applications
Mekrisuh et al. (2021) [65]	D-Mannitol (166–179 °C) Middle	Graphene nano-plates	Melting	Numerical (2D)	Optimizing geometry had better results than fins and nano-plates
Singh et al. (2021) [11]	Eutectic lithium nitrate and potassium chloride (150–200 °C) Middle	COOH-functionalized Graphene nanoplatelets (f-GNP)	Melting and solidification	Experimental and numerical (2D)	f-GNPs enhance PCM at 5% concentration
Chieruzzi et al. (2013) [66]	NaNO ₃ -KNO ₃ (223–232 °C) Middle	SiO ₂ , Al ₂ O ₃ , TiO ₂ , and SiO ₂ -Al ₂ O ₃	Melting and solidification	Experimental	1.0 wt % SiO ₂ -Al ₂ O ₃ were the most effective
Chieruzzi et al. (2017) [67]	NaNO ₃ -KNO ₃ (228.2 °C) Middle	silica (SiO ₂), alumina (Al ₂ O ₃), and SiO ₂ -Al ₂ O ₃	Melting and solidification	Experimental	Most effective were silica/alumina NPs 30 min at 200 rpm
Aslfattahi et al. (2019) [68]	NaNO ₃ -KNO ₃ (225 °C) Middle	MgO	Melting	Experimental	MgO thermally enhanced the system
Saranprabhu and Rajan (2019) [69]	NaNO ₃ -KNO ₃ (250 °C) Middle	MgO	Melting and solidification	Experimental	0.25 wt % was the best concentration of MgO
Myers et al. (2016) [70]	KNO ₃ , NaNO ₃ , KNO ₃ -NaNO ₃ Eutectic (334 °C, 306 °C, and 222 °C) Middle and High	CuO	Melting	Experimental	All showed improvement, but especially the eutectic mixture
Chieruzzi et al. (2015) [71]	KNO ₃ (334 °C) High	silica (SiO ₂), alumina (Al ₂ O ₃), and SiO ₂ -Al ₂ O ₃	Melting	Experimental	All improved but silica was significantly the best
Yaxuan et al. (2019) [72]	Eutectic mix of NaBr, KBr, LiBr, CaBr ₂ (310–314 °C) High	SiO ₂	Melting	Experimental	Factors varied with diameter and concentration
Han et al. (2020) [73]	KCl:MgCl ₂ :NaCl (3997 °C)	Al ₂ O ₃ , CuO, and ZnO	Melting	Experimental	Al ₂ O ₃ showed the best enhancement

3.2. NePCM and Fins

As discussed earlier, other heat transfer enhancement methods are commonly combined with NePCM to provide further enhancement of the LHTES system. NePCM, unlike some other enhancement methods, can be combined with nearly any type of enhancement due to the size of the particles. The following studies assessed NePCM with fins.

Hosseinzadeh et al. [74] numerically studied the enhancement of an LHTES system with branching or rectangular fins and $\text{MoS}_2\text{-TiO}_2$ NPs in water as the NePCM. The system was studied with each enhancement individually and with NPs and fins together. The tree-like fins provided better results than the rectangular fins and no fins. The inclusion of NPs without fins showed that the NPs did improve the system; however, they did not show as much of an improvement as the fins. Together, the best option for improving performance was the NPs of the highest concentration, along with the branched fins. This was significantly better than NPs alone and slightly better than branched fins alone [74].

Hajizadeh et al. [75] also studied the combination of NePCM and branched fins. The numerical study focused on the solidification of RT35 enhanced by Y-fins and CuO NPs in three different cases. The cases were no fins (case one), long Y-fins on top and V-fins on bottom (case two), and V-fins on top with Y-fins on bottom (case three), as shown in Figure 10. The first case was tested with two volume fractions of nanofluid, and the second and third were tested with and without NPs. The system without fins was the least efficient, and case two was more efficient than case three. As a result of buoyancy effects, case two was also more affected by the NP dispersion than case three. The amount of energy decreased with an increase of NPs, but case two stored more energy than case three [75].

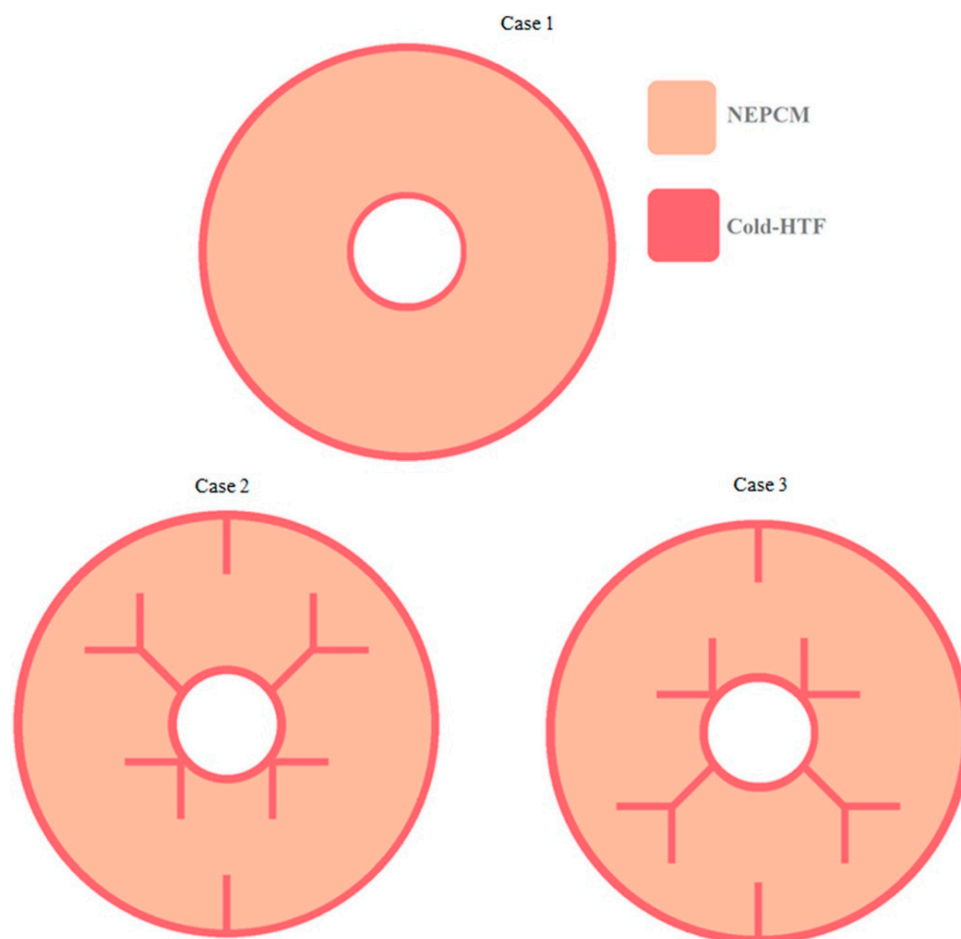


Figure 10. Fin configurations for the three cases studied by Hajizadeh et al. (Copyright 2020 Elsevier) [75].

CuO seems to be a popular choice for NPs when combined with fins. Nakhci et al. [76] studied stair-shaped fins and CuO NPs in an LHTES system with lauric acid PCM. No difference was found for the orientation of the fins (upward or downward stairs) early on; however, later in melting, natural convection affected the two orientations differently. Over-

all, the downward stair fins had a shorter melting time due to more uniform temperatures. More fins reduced the melting time but also reduced the total storage capacity, and the same resulted from thicker fins. NPs along with fins improved the melting performance. Smaller stair ratios caused initially faster melting but slower melting later. An increased stair ratio improved the energy storage capacity [76]. Copper oxide particles were chosen also by Li et al. [77], who examined the charging process of paraffin PCM with different sizes and configurations of Y-shaped fins. Six different cases of fins were studied. As is demonstrated in Figure 11, the fourth case, with long, thin fins alternating attachment to the outer and inner wall, was the best case. The worst case was case one, with short fins attached only to the inner wall. Longer, thinner fins allowed for natural convection, accelerating the melting [77].

Instead of rectangular or branched fins, Ren et al. [78] numerically studied the effects of using triangular fins, along with copper NPs, as enhancements for N-eicosane PCM. The two triangle fins were compared with one rectangle fin with the same total volume, which showed that the triangle fins melted more PCM under the same conditions. Comparing different fin lengths, longer fins improved the system, and triangle fins of each length were better than their rectangular counterparts. The melting rate was also improved by the addition of NPs, with greater concentrations producing better results, although the pure PCM with triangle fins was still better than the NePCM with a rectangular fin. However, the greater the percentage of NPs, the less of a difference there was between the two types of fins. NePCM was further studied with the triangular fins, which showed that the long, narrow fins with unequal lengths (longer on bottom and shorter on top, to enhance convection on top and conduction on the bottom) greatly improved the NePCM melting rate [78].

Copper fins are also a popular choice, even with other types of NPs. Mahdi et al. [79] used a triplex tube heat exchanger for the simultaneous charging and discharging of PCM, with an outer tube of cold HTF, a middle tube of RT82 PCM with copper fins extending into it, and an inner tube of hot HTF. Simultaneous charging and discharging is a likely real-world scenario that is not often studied. They numerically studied different fin setups and enhancement with Al_2O_3 for the system. Adding fins caused natural convection to assist in melting the bottom half of the PCM, where without fins, natural convection would only occur in the top half. Adding V-shaped fins in the bottom half also improved melting. Since it simultaneously charged and discharged, optimization was based on the final steady-state time and final steady-state liquid fraction of the system. NPs provided very little enhancement to the system in comparison to the fins, so they were considered to be unnecessary [79]. Bondareva et al. [80] also used copper fins and alumina NPs to enhance the thermal performance of an LHTES system. They tested various PCMs with NPs and fins as heat sinks for electronics. The rectangular, two-dimensional numerical model with copper fins was heated by a constant source underneath. The liquid volume fraction versus time for the five PCMs tested (n-octadecane, capric acid, lauric acid, RT-50, and RT-80) is shown in Figure 12. Since n-octadecane has the lowest melting point, it started melting first; however, since it melted quickly, it only cooled for a short amount of time. The lauric acid had the lowest temperature heat sink after four minutes, making it the best choice. NPs reduced latent heat, accelerated the melting process, and reduced the overall heat capacity. As a result of this, NPs only enhanced the system up to 2% concentration, which was determined to be the best concentration [80].

Copper and copper oxide seem to be very common and effective materials for fin-NP enhanced LHTES systems. What is lacking is combinations of other fin and NP materials. Some studies also found that in comparison to fins, the NPs were an unnecessary enhancement. This was not the case with all of the studies, and perhaps it was due to the type of NP used in combination with the PCM and melting temperature of the system. Further studies of those systems with other NP materials could be conducted. Additionally, there seems to be a lack of middle and high temperature studies with NPs and fins as well as a lack of experimental studies. A majority—if not all—of these studies with NPs

and fins are conducted numerically. Experimental studies should be conducted in the future. Table 2 summarizes the studies that used NePCM combined with fins to enhance LHTES system.

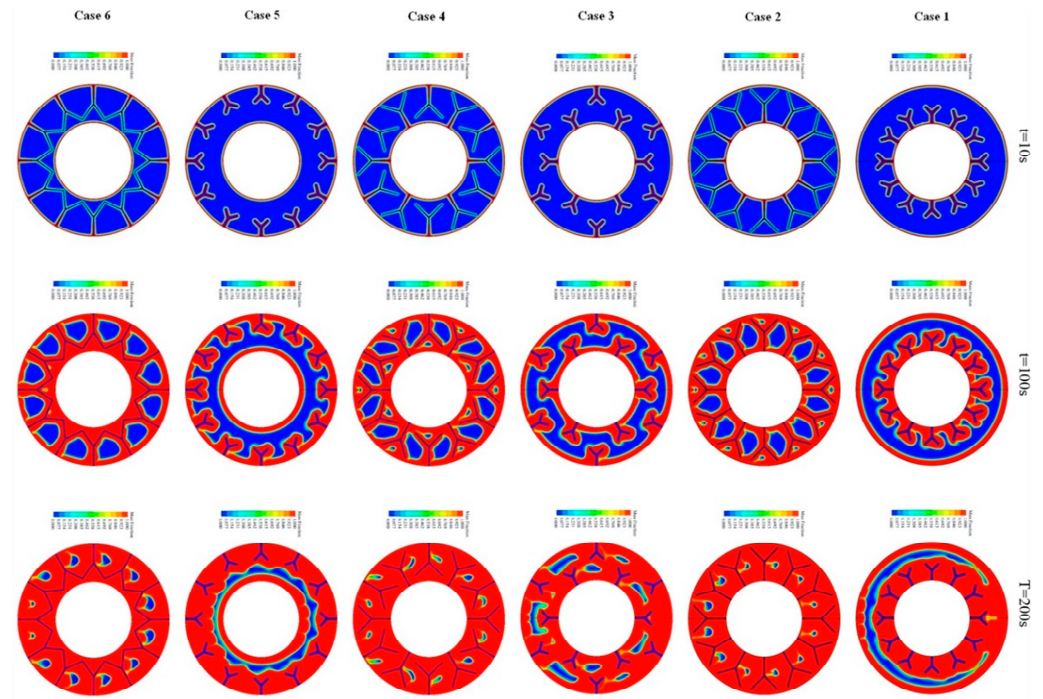


Figure 11. The liquid fraction in the six different cases at different times. (Copyright 2020 Elsevier) [80].

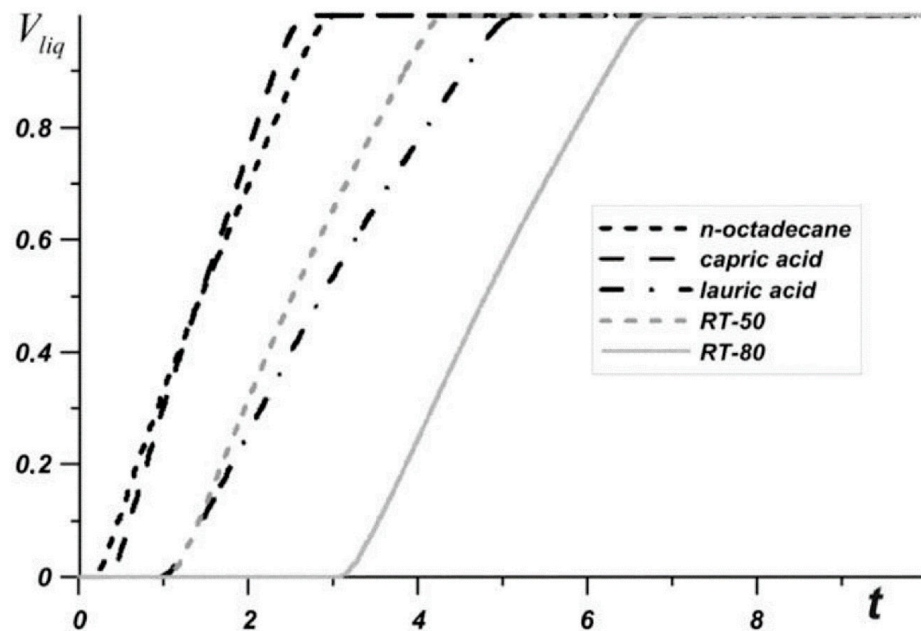


Figure 12. Liquid volume fraction over time for the different PCMs tested by Bondareva et al. (Copyright 2020 Bondareva et al. <https://creativecommons.org/licenses/by/4.0/legalcode>) Accessed on 18 June 2021 [80].

Table 2. A summary of studies that used NePCM combined with fins to enhance LHTES system.

Authors	PCM Melting Point (°C)	Nanoparticle Type/ Enhancement Method(s)	Phase Change Process	Study Case	Result
Hosseinzadeh et al. (2021) [74]	Water (0 °C) Low	MoS ₂ -TiO ₂ and branched fins	Solidification	Numerical (2D)	High NP concentration with branched fins were the best enhancement technique
Hajizadeh et al. (2020) [75]	RT35 (35 °C) Low	CuO and branched fins	Solidification	Numerical (2D)	NP improved all cases, case 2 worked best
Nakhachi et al. (2021) [76]	Lauric acid (43.4–48.1 °C) Low	CuO and stair fins	Melting	Numerical (2D)	NP and stair fins improved melting
Li et al. (2021) [77]	Paraffin (n-octadecane) Low	Copper oxide and fins	Melting	Numerical (2D)	Long, thin fins from both walls worked best
Ren et al. (2019) [78]	N-eicosane (35.85 °C) Low	Copper and triangle fins	Melting	Numerical (2D)	Triangle fins and NP improved system
Mahdi et al. (2019) [79]	RT82 (77–85 °C) Low	Al ₂ O ₃ and copper fins	Simultaneous charging and discharging	Numerical (2D)	Fins and their geometry had greater effects than the NPs
Bondareva et al. (2020) [80]	n-Octadecane (28.05 °C), Capric acid (32 °C), Lauric acid (46 °C), RT-50 (49 °C), RT-80 (81 °C) Low	Al ₂ O ₃ and fins	Melting	Numerical (2D)	NPs enhanced up to 2% concentration

3.3. NePCMs and Heat Pipes

Although fins can be used alone, they are often added to heat pipes. This triple combination of fins, heat pipes, and NPs was studied by Koukou et al. [81]. They experimentally studied the melting and solidification of A44 paraffin enhanced with GNPs and finned heat pipes in a small LHTES unit. They also tested the effects of the NPs and HTF flow rate. DSC was used to find thermal properties, and thermocouples measured temperatures during melting and solidification. HTF flow rates of 30, 45, and 60 L/h were tested, with faster flow rates leading to faster melting. For the NePCM, the thermocouples were replaced with thermistors, as the ultrasonic agitation was applied to keep the NP suspended interfered with the thermocouples. The NPs reduced time for both charging and discharging and made it more efficient. An issue occurred during solidification where NePCM coated the heat pipes and impeded heat transfer; however, this was easily overcome by slowing the HTF initially and then speeding it up throughout solidification [81]. Mahdavi et al. [82] conducted a numerical simulation of just heat pipes and NPs, using a two-dimensional axisymmetric model in ANSYS-FLUENT. In the model, the PCM Rubitherm 55 was used in a shell-and-tube LHTES system. Various types of enhancements were tested for their effects on the overall system performance, particularly melting and solidification times and the system capacity to store and release energy. The enhancements included horizontal heat pipes, the addition of different types of NPs, and different NP concentrations. The heat pipes significantly decreased the amount of time required for melting and solidification, therefore improving the overall performance, as shown in Figure 13. The time for a full charge decreased from 2100 min without heat pipes to 341 min with four heat pipes. For four heat pipes, 95% of the PCM melted in 169 min, so if only 95% capacity is needed, the charging time can be cut in half. Discharging time decreased by 96% with four heat pipes compared to none. The 14% decrease in storage capacity due to the heat pipes is

very worth it for these significant improvements. The NP concentration increasing also decreased the melting and solidification times and the amount of energy that could be stored. The differences between NP types depended on the number of heat pipes, with fewer heat pipes resulting in a bigger difference between types. In the case with fewer heat pipes, silver was the best NP type. Overall, the heat pipes provided more significant results than the addition of NPs [82].

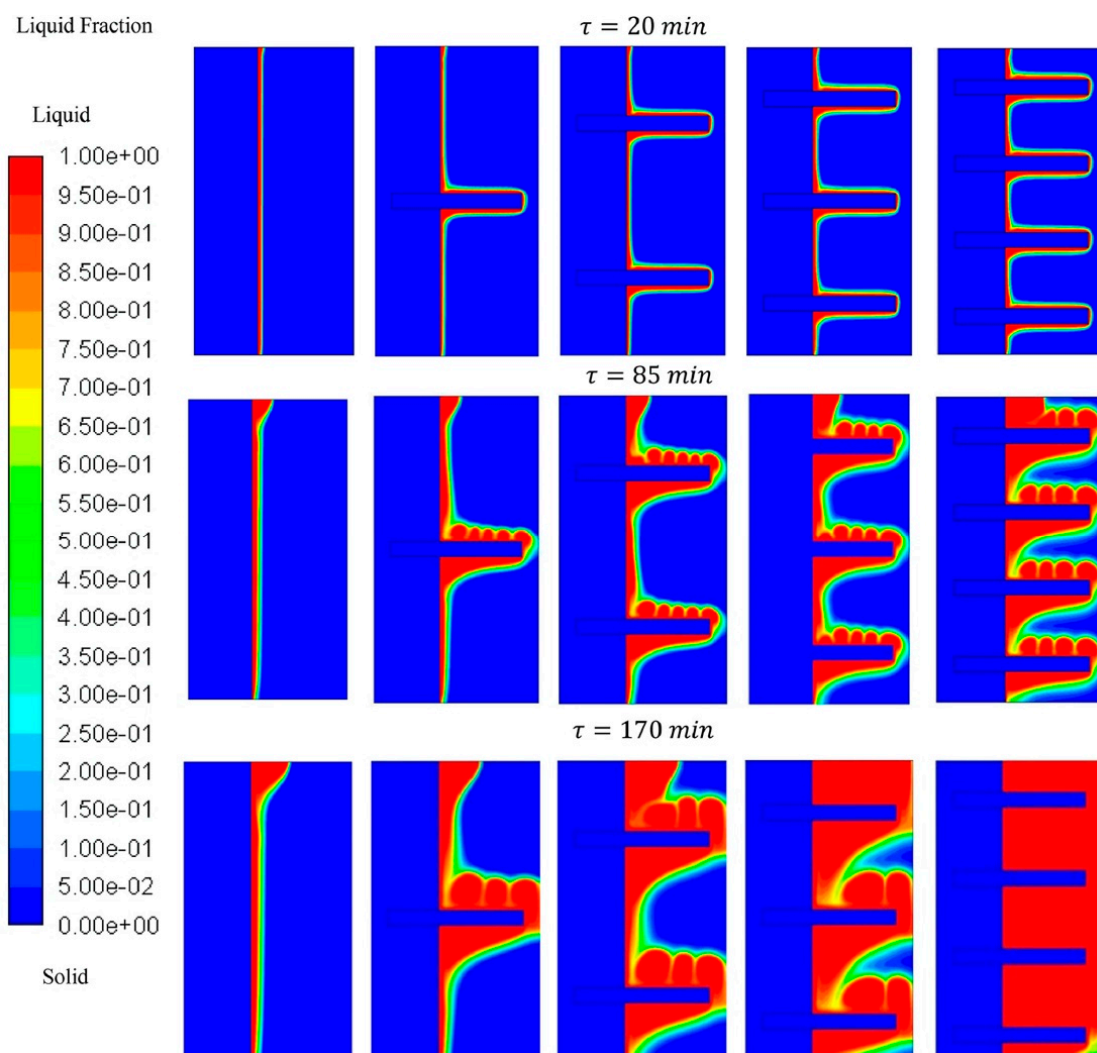


Figure 13. The PCM liquid fractions at three different times with the different numbers of heat pipes. (Copyright 2019 Elsevier) [82].

Another study by Mahdavi et al. [83] numerically investigated a low temperature, shell and tube LHTES system of RT-55 PCM enhanced with heat pipes and Cu, CuO, Al₂O₃, or Ag NPs. The number of heat pipes, NP volume fraction, and types of NPs were all compared. Increasing the number of heat pipes decreased the melting time and created a more uniform heat distribution. An increased volume fraction of NPs decreased the melting time; however, it also increased the viscosity and decreased the total heat stored. Silver had the best results of the types of NPs; however, the type of particle was not significant in the end [83].

A study by Tiari et al. [84] looked at high-temperature PCM with finned heat pipes and NPs. They numerically investigated the effects of copper oxide and aluminum oxide NPs on the melting of potassium nitrate, which is a high-temperature PCM (335 °C melting temperature). The two-dimensional model included finned heat pipes in a square PCM container. Constant heat flux was applied to the bottom of the container to melt the PCM.

An increased number of heat pipes led to shorter melting times. Three heat pipes were used in the case where different amounts of copper NPs were tested. Melting began faster with the Cu particles, and increasing the amount greatly sped up the melting process and reduced the total melting times. The enhancement above 5% NPs was insignificant, while increased viscosity decreased performance. In comparison, the aluminum oxide particles had only a slightly higher melting rate than the Cu particles, which was insignificant [84]. A similar study was conducted by the same authors on the solidification of a high-temperature LHTES system with potassium nitrate PCM enhanced by copper oxide and aluminum oxide NPs. Different types and volume fractions of NPs along with the number of finned heat pipes were compared. Results showed that an increase in heat pipes increased the solidification rate and decreased the total solidification time. The volume fraction of NPs was studied with copper oxide particles and three heat pipes. Results showed that adding 2% NPs led to a large reduction in solidification time, but the reductions between 2%, 5%, and 10% volume fractions were not as significant. This showed that above 2%, the benefits of higher volume fraction decreased, which was due to increased viscosity. There was not a significant difference between the two NP types [85]. Another high-temperature study by Ren et al. [86] numerically investigated the effects of changing different factors of the enhancements on an LHTES system. The heat pipes, copper foam, and copper NPs were tested at different radii, porosity/pore sizes, and volume fractions, respectively. Each case was compared by melting fraction, energy stored (per unit width), and average temperature. The decreased porosity of the metal foam and increased volume fraction of NPs both increased the melting time with the tradeoff of decreased energy storage. Larger heat pipes also improved melting but decreased the energy storage. As a result of differing heat transfer mechanisms, the average temperature behaved differently at different foam porosities. At high porosity, it increased with a decrease in pore size due to conduction, but this effect lessened at low porosities, since the metal inhibited convection. When testing NPs and foam against each other, it was found that the metal foam had a more efficient enhancement than the NPs [86].

As with the fins, some studies found that the NPs were insignificant in comparison to the enhancement of the heat pipes. However, others found them to still be effective with the heat pipes, and all studies reported some sort of enhancement with the NPs, no matter the type or melting temperature. Overall, it seems useful to look into this combination in the future, perhaps considering different NP types in each individual scenario. Table 3 summarizes the studies that used NePCM combined with heat pipes to enhance LHTES system.

Table 3. A summary of studies that used NePCM combined with heat pipes to enhance the LHTES system.

Authors	PCM Melting Point (°C)	Nanoparticle Type/ Enhancement Method(s)	Phase Change Process	Study Case	Result
Koukou et al. (2019) [81]	Paraffin (A44) (44 °C) Low	Graphite nano-platelets and finned heat pipes	Melting and solidification	Experimental	NPs reduced charging and discharging times
Mahdavi et al. (2020) [82]	Rubitherm 55 (51–57 °C) Low	Aluminum oxide, silver, copper, and copper oxide NPs and horizontal heat pipes	Melting and solidification	Numerical (2D)	More heat pipes and more NP decreased time, decreased storage capacity
Mahdavi et al. (2018) [83]	Rubitherm 55 (51–57 °C) Low	Cu, CuO, Al ₂ O ₃ , Ag, and heat pipes	Melting	Numerical (2D)	Enhancements improved melting, but type of NP was insignificant

Table 3. Cont.

Authors	PCM Melting Point (°C)	Nanoparticle Type/ Enhancement Method(s)	Phase Change Process	Study Case	Result
Tiari et al. (2018) [84]	Potassium nitrate (335 °C) High	CuO and Al ₂ O ₃ , finned heat pipes	Melting	Numerical (2D)	Increased concentration of NP improved melting, type did not matter
Tiari et al. (2019) [85]	Potassium nitrate (335 °C) High	CuO and Al ₂ O ₃ and finned heat pipes	Solidification	Numerical (2D)	NP improved the system up to 2% volume fraction, which was the same for either NP type
Ren et al. (2018) [86]	Li ₂ CO ₃ -K ₂ CO ₃ (485.85 °C) High	Cu, metal foam, heat pipes	Melting	Numerical (2D)	All enhancements improved the system w/tradeoff of decreased storage

3.4. Highly Conductive Porous Materials Impregnated with NePCMs

It is not only Ren et al. [86] who found that regular NPs were less effective than the addition of foam. Yu et al. [87] attempted to fix the issue of NPs settling by the addition of a dispersing agent and use of ultrasonic dispersion. Carbon graphite foam was used along with spherical AlN (aluminum nitride), one-dimensional tubular carbon nanotubes, or two-dimensional sheet shaped graphene NPs (GnPs) to enhance acetamide PCM. Oleic acid was chosen to disperse the NPs, and the improved dispersion also increased the thermal conductivity. Even with the oleic acid preventing particles from sinking, microscopic aggregates still formed, so ultrasound was used to break particles apart. The relation between time of ultrasound and size of NPs was studied with a particle-size analyzing laser to find volumes. The particles were well-dispersed at 90 min, after which the ultrasound did not make much of a difference. A two-dimensional numerical study was also conducted using ANSYS, with graphene sheets or “virtual particles” (with the same properties other than shape) and acetamide. The GnPs formed thermally conductive pathways, so they had a much greater enhancement effect than the virtual particles. Carbon foam was also tested numerically to compare to the experimental results, which followed the same upward thermal conductivity trend [87].

Other than Ren et al., most low-temperature PCM studies with foam used paraffin-based PCMs. Senobar et al. [88] experimentally tested PCM alone, with NPs, with metal foam, and with both to see which setup was the most effective. The PCM used was RT44HC, with CuO NPs and copper foam. First, a constant temperature heat source was implemented to test melting and solidification; then, a constant flux heat source was used during melting. Both the NPs and metal foam showed improvement over the pure PCM, with the foam being the most effective. The combination of NP and metal foam was not as effective as foam alone. Effectiveness was measured by reduction in melting and solidification times. NPs were also shown to cause hollow portions inside of the solidified PCM. The enhancements were much more effective with the constant temperature heat source than flux. It was concluded that metal foam alone was the best enhancement [88]. Buonomo et al. [89] numerically studied an LHTES system with RT 58 PCM, aluminum foam, heat pipes, and aluminum oxide NPs. The NPs alone showed very little improvement over the pure PCM. The metal foam significantly improved the system, and the system with nano-PCM in metal foam had the quickest melting time of all the systems. The foam did have the drawback of decreasing the energy storage capacity [89].

Ma et al. [90] also experimentally studied paraffin but enhanced with expanded graphene and NPs. The samples included copper, aluminum, iron, and nickel particles

each at five different weight percentages. Ultrasonic oscillation was used to prevent sinking and the agglomeration of particles. The ideal amount of expanded graphene (EG) was found to be 11% to prevent PCM leakage and also have a good heat capacity. Copper and aluminum NPs were the most compatible with the paraffin. Thermal conductivity increased with the addition of NPs, with Cu being the best at 1.95 W/mK for a mass fraction of 1.9% (compared to 0.216 W/mK without any enhancements and 1.073 W/mK with EG), and thermal conductivity was linked directly to temperature. Heat storage speed was accelerated, and heat storage capacity was strengthened with the addition of the Cu particles [90].

In a middle-temperature application, Kim et al. [91] experimentally tested erythritol PCM with carbon foam and several different NPs. The NPs tested were Ag, Al, CNTs, and graphene NPs. The foam, which was impregnated with PCM using the vacuum method, was in an air-tight glass container submerged in a hot oil bath, and the temperature of the PCM was tracked with a thermocouple. All NP-foam combinations enhanced thermal conductivity when compared to carbon foam without NPs. Enhancement in thermal conductivity ranged from 150 to 225%, with Ag, Al, CNT, and graphene increasing in that order. Melting time also decreased, in the same order with graphene as the fastest melting time. Latent heat was reduced with the addition of foam but stayed relatively the same with the addition of the NPs; however, latent heat loss during thermal cycling was lower with the foam [91].

Yu et al. [92] made a high-temperature PCM with the combination of MgCl_2 , NaCl, and KCl, which was enhanced with expanded graphite and SiO_2 NPs. Expanded graphite was shown to decrease the leakage of PCM greatly as well as increase the thermal conductivity. The addition of SiO_2 NPs increased the specific heat and the thermal conductivity of the PCM, with an increase of 23.2 times in the solid state and 9.2 times in the liquid state, and thermal cycling showed great thermal stability [92].

The above studies often seemed to find that the addition of metal foam was a more effective enhancement than NPs. While this does not mean that NPs are not a viable enhancement, it is important to try to understand why the foams may have been more effective in these studies. Although foams may have performed better at heat transfer in these studies, NPs take up much less space than metal foams, therefore causing less of a decrease in thermal storage capacity. It is theorized in [87] that the conductive pathway formed by the sheet-shaped graphene NPs made them more effective. It is probable that the pathways formed by the foam make it easier for heat to transfer than singular NPs. A potential solution to this is changing the shapes of NPs in order to better form these pathways. It can also be considered that the tradeoff of larger thermal storage capacity is enough in certain situations to make NPs a better choice than foams. The topic of NP shapes is a potential future research topic to enhance the effects of NePCM. Table 4 summarizes the studies that used NePCM combined with highly conductive porous media to enhance LHTES system.

Table 4. A summary of studies that used NePCM combined with highly conductive porous media to enhance the thermal performance of LHTES systems.

Authors	PCM Melting Point (°C)	Nanoparticle Type/ Enhancement Method(s)	Phase Change Process	Study Case	Result
Yu et al. (2016) [87]	Acetamide (Not Reported) Low	Nano-AlN, carbon nanotubes and graphene and carbon graphite foam	N/A	Experimental and numerical (2D)	Dispersion techniques improved thermal conductivity
Senobar et al. (2020) [88]	RT44HC (41–44 °C) Low	Copper oxide NPs and copper foam	Melting and solidification	Experimental	Metal foam alone was the best enhancement

Table 4. Cont.

Authors	PCM Melting Point (°C)	Nanoparticle Type/ Enhancement Method(s)	Phase Change Process	Study Case	Result
Buonomo et al. (2018) [89]	RT 58 Paraffin (48–62 °C) Low	Aluminum oxide NP, aluminum foam, heat pipes	Melting	Numerical (3D)	Metal foam enhanced more than NPs; their combination was best.
Ma et al. (2020) [90]	Paraffin (28–37 °C) Low	Cu, Al, Fe, and Ni NPs. Expanded graphite porous material	Melting	Experimental	Cu were the best and the EG prevented leakage
Kim et al. (2019) [91]	Erythritol (120 °C) Middle	Ag, Al, carbon nanotubes, and graphene NPs, with carbon foam	Melting and solidification	Experimental	All were effective, with graphene as the best enhancement
Yu et al. (2021) [92]	MgCl ₂ -NaCl-KCl (383.5 °C) High	Expanded graphite and SiO ₂ NPs	Melting and solidification	Experimental	Both EG and NPs enhanced the system

3.5. NPs and Multiple PCMs

While it is not the most popular enhancement method, the addition of NPs into a multiple PCM LHTES system is a potential option. Mahdi et al. [93] studied the solidification of multiple PCMs enhanced with cascaded metal foam and NPs in a numerical study. The shell-and-tube energy storage system held between one and three PCMs of different melting points in different segments. There were nine cases each with a unique set of enhancements. Three sets of cases had either no enhancement, NPs, or metal foam. Each of the three sets had three cases: one PCM (RT-60), two PCMs (RT-55 and RT-65), and three PCMs (all three). The PCMs were chosen so that the average phase change temperature in each system was constant (since RT-60 was halfway between the other two). Since they tested solidification, they used conduction as the source of heat transfer. The multiple PCMs were more uniform and much faster in their solidification, without any enhancements. With added alumina NPs, solidification was improved further for all three cases, with even faster solidification. With the addition of the metal foam, solidification was even faster. The case with multiple PCMs and the metal foam was the most effective case [93].

To the authors' best knowledge and as stated in Mahdi et al. [93], no other studies exist yet that combine the multiple PCM and NP enhancement techniques. This gap in the literature is one that warrants further investigation. Both enhancements were effective and should be studied also for melting, with other types of NPs and for different applications. Table 5 summarizes the studies that used multiple PCMs to enhance LHTES system.

Table 5. PCM, NP type, and enhancements are described for the multiple PCM enhanced experiment. Phase change process, type of study, and a summary of study results are also indicated.

Authors	PCM Melting Point (°C)	Enhancement Method(s)	Phase Change Process	Study Case	Result
Mahdi et al. (2020) [93]	RT-55 (51–57 °C) RT-60 (55–61 °C) RT-65 (58–67 °C)	Al ₂ O ₃ NPs, metal foam (Al6061), and multiple PCMs	Solidification	Numerical (2D)	All showed enhancement, with multiple PCM and metal foam the best

4. Conclusions

In the current literature, the most commonly studied NePCM by far is paraffin-based PCM. Likely due to its low cost and wide variety of melting temperatures, this low-temperature PCM is used in all types of studies. Other commonly used PCMs include water, NaNO_3 - KNO_3 mixture, KNO_3 , chloride mixtures, PEG, erythritol as a middle temperature PCM, and fatty acids, especially lauric, capric, and palmitic. The most common NP type is Al_2O_3 , which is followed by copper, copper oxide, carbon-based, SiO_2 , and many others, usually metals and metal oxides.

Comparing NP types for NePCM can be tricky. The “best” NP type is highly dependent on the individual situation, including melting temperature, type of PCM, and other applied enhancement methods. There appears to be no strong pattern between the best NPs in each study. For example, Al_2O_3 is generally accepted as a good NP for NePCM; however, studies showed that certain particles occasionally worked better, and sometimes, these Al_2O_3 particles sank. The treatment of these NPs to create a more consistent performance in LHTES systems is an unexplored area for potential future work.

The density of the PCM used can affect whether NPs sink. Some studies even used stirring during or between cycles to prevent sinking, keep an even distribution, and prevent agglomeration. This was effective in accomplishing those goals; however, it does take energy. One benefit of NPs dispersion as a heat transfer enhancement is its passive nature. Adding in a stirring step adds an active element to this enhancement, requiring external energy to be used. Since the goal of LHTES is to store energy, using energy for this purpose may not be the ideal solution.

The addition of other enhancements such as metal foam, fins, heat pipes, and multiple PCMs to NePCM has shown to be beneficial to the systems. Many studies found that the NPs further enhance these systems. However, some studies did find the effects of NPs to be weak compared to the other enhancements. This was the case for some—but certainly not all—of the cases with metal foams, heat pipes, and fins. Multiple PCMs should be studied further to better test the effects of adding NPs.

A potential reason for the cases that found NPs to have a weaker effect is that other techniques form conductive pathways that transfer heat faster than spherical NPs. Conductive pathways cannot be formed by spherical NPs, as the addition of too many NPs caused an agglomeration of particles that hinders their enhancement ability. One possible solution is to test more NPs of different shapes, as some of the studies here have done. Longer and thinner particles seem to have this ability to form conductive pathways, which is something that should be studied in the future. Another issue found was that sometimes with metal foams and NPs, the particles can cause hollow portions in the PCM. Finding the root of and remedying this issue is another potential future work.

Other potential future work includes studying different shapes of NPs. Some studies have begun looking into this. For example, carbon is a great enhancement, and it seems as though the shape affects how well it works. MWCNTs seem to be more effective than plain graphite particles. Other gaps in the literature include middle and high-temperature NePCMs and combining with other enhancements. Most current studies used low-temperature NEPCM, so looking further into higher temperatures is important in the future. There are also fewer studies that combine NPs with other enhancements than there are of just NPs alone. Another future work could be establishing the effectiveness of different NPs at different temperatures to search for patterns.

Author Contributions: Investigation, K.T.; supervision, S.T.; writing—original draft, K.T.; writing—review and editing, S.T. All authors have read and agreed to the published version of the manuscript.

Funding: This research received no external funding.

Acknowledgments: The authors would like to thank Gannon University for supporting this work.

Conflicts of Interest: The authors declare no conflict of interest.

References

1. Sarbu, I.; Sebarchievici, C. A comprehensive review of thermal energy storage. *Sustainability* **2018**, *10*, 191. [CrossRef]
2. Khan, Z.; Khan, Z.; Ghafoor, A. A review of performance enhancement of PCM based latent heat storage system within the context of materials, thermal stability and compatibility. *Energy Convers. Manag.* **2016**, *115*, 132–158. [CrossRef]
3. Tiari, S.; Qiu, S. Three-dimensional simulation of high temperature latent heat thermal energy storage system assisted by finned heat pipes. *Energy Convers. Manag.* **2015**, *105*, 260–271. [CrossRef]
4. De Gracia, A.; Cabeza, L.F. Phase change materials and thermal energy storage for buildings. *Energy Build.* **2015**, *103*, 414–419. [CrossRef]
5. Jiang, Z.Y.; Qu, Z.G. Lithium-ion battery thermal management using heat pipe and phase change material during discharge-charge cycle: A comprehensive numerical study. *Appl. Energy* **2019**, *242*, 378–392. [CrossRef]
6. Tariq, S.L.; Ali, H.M.; Akram, M.A.; Janjua, M.M.; Ahmadlouydarab, M. Nanoparticles enhanced phase change materials (NePCMs)-A recent review. *Appl. Therm. Eng.* **2020**, *176*, 115305. [CrossRef]
7. European Energy Research Alliance. *High-Temperature Latent Heat Storage [digital]*; EERA: Brussels, Belgium, 2018; Available online: <https://eera-es.eu/> (accessed on 18 June 2021).
8. Huang, Z.; Xie, N.; Luo, Z.; Gao, X.; Fang, X.; Fang, Y.; Zhang, Z. Characterization of medium-temperature phase change materials for solar thermal energy storage using temperature history method. *Sol. Energy Mater. Sol. Cells* **2018**, *179*, 152–160. [CrossRef]
9. Sharma, A.; Tyagi, V.V.; Chen, C.R.; Buddhi, D. Review on thermal energy storage with phase change materials and applications. *Renew. Sustain. Energy Rev.* **2009**, *13*, 318–345. [CrossRef]
10. Raj, C.R.; Suresh, S.; Singh, V.K.; Bhavsar, R.R.; Chandrasekar, M.; Archita, V. Life cycle assessment of nanoalloy enhanced layered perovskite solid-solid phase change material till 10000 thermal cycles for energy storage applications. *J. Energy Storage* **2021**, *35*, 102220. [CrossRef]
11. Singh, R.P.; Sze, J.Y.; Kaushik, S.C.; Rakshit, D.; Romagnoli, A. Thermal performance enhancement of eutectic PCM laden with functionalised graphene nanoplatelets for an efficient solar absorption cooling storage system. *J. Energy Storage* **2021**, *33*, 102092. [CrossRef]
12. Mehta, D.S.; Solanki, K.; Rathod, M.K.; Banerjee, J. Thermal performance of shell and tube latent heat storage unit: Comparative assessment of horizontal and vertical orientation. *J. Energy Storage* **2019**, *23*, 344–362. [CrossRef]
13. Mahdavi, M.; Qiu, S.; Tiari, S. Improvement of a novel heat pipe network designed for latent heat thermal energy storage systems. *Appl. Therm. Eng.* **2016**, *108*, 878–892. [CrossRef]
14. Tiari, S.; Mahdavi, M.; Qiu, S. Experimental study of a latent heat thermal energy storage system assisted by a heat pipe network. *Energy Convers. Manag.* **2017**, *153*, 362–373. [CrossRef]
15. Tiari, S.; Qiu, S.; Mahdavi, M. Numerical study of finned heat pipe-assisted thermal energy storage system with high temperature phase change material. *Energy Convers. Manag.* **2015**, *89*, 833–842. [CrossRef]
16. Tiari, S.; Qiu, S.; Mahdavi, M. Discharging process of a finned heat pipe-assisted thermal energy storage system with high temperature phase change material. *Energy Convers. Manag.* **2016**, *118*, 426–437. [CrossRef]
17. Aly, K.A.; El-Lathy, A.R.; Fouad, M.A. Enhancement of solidification rate of latent heat thermal energy storage using corrugated fins. *J. Energy Storage* **2019**, *24*, 100785. [CrossRef]
18. Tiari, S.; Hockins, A.; Mahdavi, M. Numerical study of a latent heat thermal energy storage system enhanced by varying fin configurations. *Case Stud. Therm. Eng.* **2021**, *25*, 100999. [CrossRef]
19. Gasia, J.; Maldonado, J.M.; Galati, F.; de Simone, M.; Cabeza, L.F. Experimental evaluation of the use of fins and metal wool as heat transfer enhancement techniques in a latent heat thermal energy storage system. *Energy Convers. Manag.* **2019**, *184*, 530–538. [CrossRef]
20. Reyes, A.; Negrete, D.; Mahn, A.; Sepúlveda, F. Design and evaluation of a heat exchanger that uses paraffin wax and recycled materials as solar energy accumulator. *Energy Convers. Manag.* **2014**, *88*, 391–398. [CrossRef]
21. Tiari, S.; Mahdavi, M. Computational study of a latent heat thermal energy storage system enhanced by highly conductive metal foams and heat pipes. *J. Anal. Calorim.* **2020**, *141*, 1741–1751. [CrossRef]
22. Lakshmi Narasimhan, N. Assessment of latent heat thermal storage systems operating with multiple phase change materials. *J. Energy Storage* **2019**, *23*, 442–455. [CrossRef]
23. Li, W.Q.; Guo, S.J.; Tan, L.; Liu, L.L.; Ao, W. Heat transfer enhancement of nano-encapsulated phase change material (NEPCM) using metal foam for thermal energy storage. *Int. J. Heat Mass Transf.* **2021**, *166*, 120737. [CrossRef]
24. Dutkowski, K.; Kruzel, M. Microencapsulated PCM slurries' dynamic viscosity experimental investigation and temperature-dependent prediction model. *Int. J. Heat Mass Transf.* **2019**, *145*, 118741. [CrossRef]
25. Dutkowski, K.; Kruzel, M.; Zajackowski, B.; Białko, B. The experimental investigation of mPCM slurries density at phase change temperature. *Int. J. Heat Mass Transf.* **2020**, *159*, 120083. [CrossRef]
26. Dutkowski, K.; Kruzel, M.; Zajackowski, B. Determining the heat of fusion and specific heat of microencapsulated phase change material slurry by thermal delay method. *Energies* **2021**, *14*, 179. [CrossRef]
27. Elgafy, A.; Lafdi, K. Effect of carbon nanofiber additives on thermal behavior of phase change materials. *Carbon* **2005**, *43*, 3067–3074. [CrossRef]
28. Khodadadi, J.M.; Hosseiniadeh, S.F. Nanoparticle-enhanced phase change materials (NEPCM) with great potential for improved thermal energy storage. *Int. Commun. Heat Mass Transf.* **2007**, *34*, 534–543. [CrossRef]

29. Jourabian, M.; Farhadi, M. Melting of nanoparticles-enhanced phase change material (NEPCM) in vertical semicircle enclosure: Numerical study. *J. Mech. Sci. Technol.* **2015**, *29*, 3819–3830. [\[CrossRef\]](#)
30. Feng, Y.; Li, H.; Li, L.; Bu, L.; Wang, T. Numerical investigation on the melting of nanoparticle-enhanced phase change materials (NEPCM) in a bottom-heated rectangular cavity using lattice Boltzmann method. *Int. J. Heat Mass Transf.* **2015**, *81*, 415–425. [\[CrossRef\]](#)
31. Akhmetov, B.; Navarro, M.E.; Seitov, A.; Kaltayev, A.; Bakenov, Z.; Ding, Y. Numerical study of integrated latent heat thermal energy storage devices using nanoparticle-enhanced phase change materials. *Sol. Energy* **2019**, *194*, 724–741. [\[CrossRef\]](#)
32. Abdulateef, A.M.; Jaszczur, M.; Hassan, Q.; Anish, R.; Niyas, H.; Sopian, K.; Abdulateef, J. Enhancing the melting of phase change material using a fins–nanoparticle combination in a triplex tube heat exchanger. *J. Energy Storage* **2021**, *35*, 102227. [\[CrossRef\]](#)
33. Zaidan, M.J.; Alhamdo, M.H. Improvement in heat transfer inside a phase change energy system. *Int. J. Mech. Mechatron. Eng.* **2018**, *18*, 33–46.
34. Farsani, R.Y.; Raisi, A.; Nadooshan, A.A.; Vanapalli, S. Does nanoparticles dispersed in a phase change material improve melting characteristics? *Int. Commun. Heat Mass Transf.* **2017**, *89*, 219–229. [\[CrossRef\]](#)
35. Elbahjaoui, R.; el Qarnia, H. Transient behavior analysis of the melting of nanoparticle-enhanced phase change material inside a rectangular latent heat storage unit. *Appl. Therm. Eng.* **2017**, *112*, 720–738. [\[CrossRef\]](#)
36. Elbahjaoui, R.; el Qarnia, H. Thermal analysis of nanoparticle-enhanced phase change material solidification in a rectangular latent heat storage unit including natural convection. *Energy Build.* **2017**, *153*, 1–17. [\[CrossRef\]](#)
37. Nie, C.; Liu, J.; Deng, S. Effect of geometric parameter and nanoparticles on PCM melting in a vertical shell-tube system. *Appl. Therm. Eng.* **2021**, *184*, 116290. [\[CrossRef\]](#)
38. Hosseini, S.M.J.; Ranjbar, A.A.; Sedighi, K.; Rahimi, M. Melting of nanoparticle-enhanced phase change material inside shell and tube heat exchanger. *J. Eng.* **2013**, *2013*, 1–8. [\[CrossRef\]](#)
39. Algarni, S.; Mellouli, S.; Alqahtani, T.; Almutairi, K.; Khan, A.; Anqi, A. Experimental investigation of an evacuated tube solar collector incorporating nano-enhanced PCM as a thermal booster. *Appl. Therm. Eng.* **2020**, *180*, 115831. [\[CrossRef\]](#)
40. Nitsas, M.T.; Koronaki, I.P. Thermal analysis of pure and nanoparticle-enhanced PCM—Application in concentric tube heat exchanger. *Energies* **2020**, *13*, 3841. [\[CrossRef\]](#)
41. Aqib, M.; Hussain, A.; Ali, H.M.; Naseer, A.; Jamil, F. Experimental case studies of the effect of Al₂O₃ and MWCNTs nanoparticles on heating and cooling of PCM. *Case Stud. Therm. Eng.* **2020**, *22*, 100753. [\[CrossRef\]](#)
42. Temel, Ü.N.; Çiftçi, B.Y. Determination of thermal properties of a82 organic phase change material embedded with different type nanoparticles. Farklı Tipte Nanoparçacıklarla Katkılanan A82 Organik Faz Değiştiren Malzemenin Termal Özelliklerinin Belirlenmesi **2018**, *38*, 75–85.
43. Murugan, P.; Ganesh Kumar, P.; Kumaresan, V.; Meikandan, M.; Malar Mohan, K.; Velraj, R. Thermal energy storage behaviour of nanoparticle enhanced PCM during freezing and melting. *Phase Transit.* **2018**, *91*, 254–270. [\[CrossRef\]](#)
44. Thalib, M.M.; Manokar, A.M.; Essa, F.A.; Vasimalai, N.; Sathyamurthy, R.; Garcia Marquez, F.P. Comparative study of tubular solar stills with phase change material and nano-enhanced phase change material. *Energies* **2020**, *13*, 3989. [\[CrossRef\]](#)
45. Javadi, H.; Urchueguia, J.F.; Mousavi Ajarostaghi, S.S.; Badenes, B. Numerical study on the thermal performance of a single U-tube borehole heat exchanger using nano-enhanced phase change materials. *Energies* **2020**, *13*, 5156. [\[CrossRef\]](#)
46. Bashar, M.; Siddiqui, K. Experimental investigation of transient melting and heat transfer behavior of nanoparticle-enriched PCM in a rectangular enclosure. *J. Energy Storage* **2018**, *18*, 485–497. [\[CrossRef\]](#)
47. Khatibi, M.; Nemati-Farouji, R.; Taheri, A.; Kazemian, A.; Ma, T.; Niazmand, H. Optimization and performance investigation of the solidification behavior of nano-enhanced phase change materials in triplex-tube and shell-and-tube energy storage units. *J. Energy Storage* **2021**, *33*, 102055. [\[CrossRef\]](#)
48. Dastmalchi, M.; Boyaghchi, F.A. Exergy and economic analyses of nanoparticle-enriched phase change material in an air heat exchanger for cooling of residential buildings. *J. Energy Storage* **2020**, *32*, 101705. [\[CrossRef\]](#)
49. Pasupathi, M.K.; Alagar, K.; Stalin P, M.J.; Matheswaran, M.M.; Aritra, G. Characterization of hybrid-nano/paraffin organic phase change material for thermal energy storage applications in solar thermal systems. *Energies* **2020**, *13*, 5079. [\[CrossRef\]](#)
50. Zhou, Y.; Jiang, Y.; Liu, F.; Li, Q. Thermal conductivity and thermal mechanism of aluminum nanoparticles/octadecane composite phase change materials from molecular dynamics simulations and experimental study. *J. Ovonic Res.* **2016**, *12*, 49–58.
51. Badakhsh, A.; An, K.-H.; Park, C.W.; Kim, B.-J. Effects of biceramic AlN-SiC microparticles on the thermal properties of paraffin for thermal energy storage. *J. Nanomater.* **2018**, *2018*, 1–10. [\[CrossRef\]](#)
52. Maher, H.; Rocky, K.A.; Bassiouny, R.; Saha, B.B. Synthesis and thermal characterization of paraffin-based nanocomposites for thermal energy storage applications. *Therm. Sci. Eng. Prog.* **2021**, *22*, 100797. [\[CrossRef\]](#)
53. Ghalambaz, M.; Doostani, A.; Chamkha, A.J.; Ismael, M.A. Melting of nanoparticles-enhanced phase-change materials in an enclosure: Effect of hybrid nanoparticles. *Int. J. Mech. Sci.* **2017**, *134*, 85–97. [\[CrossRef\]](#)
54. Liang, L.; Chen, X. Preparation and thermal properties of eutectic hydrate salt phase change thermal energy storage material. *Int. J. Photoenergy* **2018**, *2018*, 1–9. [\[CrossRef\]](#)
55. Jamalabadi, M.Y.A. Use of nanoparticle enhanced phase change material for cooling of surface acoustic wave sensor. *Fluids* **2021**, *6*, 31. [\[CrossRef\]](#)
56. Marcos, M.A.; Cabaleiro, D.; Hamze, S.; Fedele, L.; Bobbo, S.; Estellé, P.; Lugo, L. NePCM based on silver dispersions in poly(ethylene glycol) as a stable solution for thermal storage. *Nanomaterials* **2019**, *10*, 19. [\[CrossRef\]](#)

57. Song, S.; Qiu, F.; Zhu, W.; Guo, Y.; Zhang, Y.; Ju, Y.; Feng, R.; Liu, Y.; Chen, Z.; Zhou, J.; et al. Polyethylene glycol/halloysite@Ag nanocomposite PCM for thermal energy storage: Simultaneously high latent heat and enhanced thermal conductivity. *Sol. Energy Mater. Sol. Cells* **2019**, *193*, 237–245. [\[CrossRef\]](#)
58. Qian, T.; Li, J.; Min, X.; Guan, W.; Deng, Y.; Ning, L. Enhanced thermal conductivity of PEG/diatomite shape-stabilized phase change materials with Ag nanoparticles for thermal energy storage. *J. Mater. Chem. A* **2015**, *3*, 8526–8536. [\[CrossRef\]](#)
59. Prabakaran, R.; Sidney, S.; Lal, D.M.; Selvam, C.; Harish, S. Solidification of graphene-assisted phase change nanocomposites inside a sphere for cold storage applications. *Energies* **2019**, *12*, 3473. [\[CrossRef\]](#)
60. Santhosh, S.; Satish, M.; Yadav, A.; Anish Madhavan, A. Thermal analysis of Fe₂O₃—Myristic acid nanocomposite for latent heat storage. *Mater. Today Proc.* **2021**, *52*, 687. [\[CrossRef\]](#)
61. Barreneche, C.; Martín, M.; la Calvo-de Rosa, J.; Majó, M.; Fernández, A.I. Own-synthesize nanoparticles to develop nano-enhanced phase change materials (NEPCM) to improve the energy efficiency in buildings. *Molecules* **2019**, *24*, 1232. [\[CrossRef\]](#)
62. Vivekananthan, M.; Amirtham, V.A. Characterisation and thermophysical properties of graphene nanoparticles dispersed erythritol PCM for medium temperature thermal energy storage applications. *Thermochim. Acta* **2019**, *676*, 94–103. [\[CrossRef\]](#)
63. Mayilvelnathan, V.; Arasu, A.V. Experimental investigation on thermal behavior of graphene dispersed erythritol PCM in a shell and helical tube latent energy storage system. *Int. J. Therm. Sci.* **2020**, *155*, 106446. [\[CrossRef\]](#)
64. Manickam, R.; Kalidoss, P.; Suresh, S.; Venkatachalapathy, S. Erythritol based nano-PCM for solar thermal energy storage. *Int. Res. J. Eng. Technol.* **2019**, *6*, 1631–1636.
65. u Mekrisuh, K.; Giri, S.; Udayraj; Singh, D.; Rakshit, D. Optimal design of the phase change material based thermal energy storage systems: Efficacy of fins and/or nanoparticles for performance enhancement. *J. Energy Storage* **2021**, *33*, 102126. [\[CrossRef\]](#)
66. Chieruzzi, M.; Cerritelli, G.F.; Miliozzi, A.; Kenny, J.M. Effect of nanoparticles on heat capacity of nanofluids based on molten salts as PCM for thermal energy storage. *Nanoscale Res. Lett.* **2013**, *8*, 448. [\[CrossRef\]](#)
67. Chieruzzi, M.; Cerritelli, G.F.; Miliozzi, A.; Kenny, J.M.; Torre, L. Heat capacity of nanofluids for solar energy storage produced by dispersing oxide nanoparticles in nitrate salt mixture directly at high temperature. *Sol. Energy Mater. Sol. Cells* **2017**, *167*, 60–69. [\[CrossRef\]](#)
68. Aslfattahi, N.; Rahman, S.; Mohd Sabri, M.F.; Arifutzzaman, A. Experimental investigation of thermal stability and enthalpy of eutectic alkali metal solar salt dispersed with MgO nanoparticles. *IJTech* **2019**, *10*, 1112. [\[CrossRef\]](#)
69. Saranprabhu, M.K.; Rajan, K.S. Magnesium oxide nanoparticles dispersed solar salt with improved solid phase thermal conductivity and specific heat for latent heat thermal energy storage. *Renew. Energy* **2019**, *141*, 451–459. [\[CrossRef\]](#)
70. Myers, P.D.; Alam, T.E.; Kamal, R.; Goswami, D.Y.; Stefanakos, E. Nitrate salts doped with CuO nanoparticles for thermal energy storage with improved heat transfer. *Appl. Energy* **2016**, *165*, 225–233. [\[CrossRef\]](#)
71. Chieruzzi, M.; Miliozzi, A.; Crescenzi, T.; Torre, L.; Kenny, J.M. A new phase change material based on potassium nitrate with silica and alumina nanoparticles for thermal energy storage. *Nanoscale Res. Lett.* **2015**, *10*, 984. [\[CrossRef\]](#)
72. Xiong, Y.; Wang, Z.; Wu, Y.; Xu, P.; Ding, Y.; Chang, C.; Ma, C. Performance enhancement of bromide salt by nano-particle dispersion for high-temperature heat pipes in concentrated solar power plants. *Appl. Energy* **2019**, *237*, 171–179. [\[CrossRef\]](#)
73. Han, D.; Lougou, B.G.; Xu, Y.; Shuai, Y.; Huang, X. Thermal properties characterization of chloride salts/nanoparticles composite phase change material for high-temperature thermal energy storage. *Appl. Energy* **2020**, *264*, 114674. [\[CrossRef\]](#)
74. Hosseinzadeh, K.; Erfani Moghaddam, M.A.; Asadi, A.; Mogharrebi, A.R.; Jafari, B.; Hasani, M.R.; Ganji, D.D. Effect of two different fins (longitudinal-tree like) and hybrid nano-particles (MoS₂-TiO₂) on solidification process in triplex latent heat thermal energy storage system. *Alex. Eng. J.* **2021**, *60*, 1967–1979. [\[CrossRef\]](#)
75. Hajizadeh, M.R.; Keshteli, A.N.; Bach, Q.-V. Solidification of PCM within a tank with longitudinal-Y shape fins and CuO nanoparticle. *J. Mol. Liq.* **2020**, *317*, 114188. [\[CrossRef\]](#)
76. Nakhchi, M.E.; Hatami, M.; Rahmati, M. A numerical study on the effects of nanoparticles and stair fins on performance improvement of phase change thermal energy storages. *Energy* **2021**, *215*, 119112. [\[CrossRef\]](#)
77. Li, F.; Almarashi, A.; Jafaryar, M.; Hajizadeh, M.R.; Chu, Y.-M. Melting process of nanoparticle enhanced PCM through storage cylinder incorporating fins. *Powder Technol.* **2021**, *381*, 551–560. [\[CrossRef\]](#)
78. Ren, Q.; Xu, H.; Luo, Z. PCM charging process accelerated with combination of optimized triangle fins and nanoparticles. *Int. J. Therm. Sci.* **2019**, *140*, 466–479. [\[CrossRef\]](#)
79. Mahdi, J.M.; Lohrasbi, S.; Ganji, D.D.; Nsofor, E.C. Simultaneous energy storage and recovery in the triplex-tube heat exchanger with PCM, copper fins and Al₂O₃ nanoparticles. *Energy Convers. Manag.* **2019**, *180*, 949–961. [\[CrossRef\]](#)
80. Bondareva, N.S.; Gibanov, N.S.; Sheremet, M.A. Computational study of heat transfer inside different PCMs enhanced by Al₂O₃ nanoparticles in a copper heat sink at high heat loads. *Nanomaterials* **2020**, *10*, 284. [\[CrossRef\]](#)
81. Koukou, M.K.; Dogkas, G.; Vrachopoulos, M.G.; Konstantaras, J.; Pagkalos, C.; Lymperis, K.; Stathopoulos, V.; Evangelakis, G.; Prouskas, C.; Coelho, L.; et al. Performance evaluation of a small-scale latent heat thermal energy storage unit for heating applications based on a nanocomposite organic PCM. *ChemEngineering* **2019**, *3*, 88. [\[CrossRef\]](#)
82. Mahdavi, M.; Tiari, S.; Pawar, V. A numerical study on the combined effect of dispersed nanoparticles and embedded heat pipes on melting and solidification of a shell and tube latent heat thermal energy storage system. *J. Energy Storage* **2020**, *27*, 101086. [\[CrossRef\]](#)

83. Tiari, S.; Mahdavi, M.; Pawar, V. Heat transfer analysis of a low-temperature heat pipe-assisted latent heat thermal energy storage system with nano-enhanced PCM. In Proceedings of the ASME 2018 International Mechanical Engineering Congress and Exposition, Pittsburgh, PA, USA, 9–15 November 2018; pp. 1–10.
84. Tiari, S.; Mahdavi, M.; Thakore, V.; Joseph, S. Thermal analysis of a high-temperature heat pipe-assisted thermal energy storage system with nano-enhanced phase change material. In Proceedings of the ASME 2018 International Mechanical Engineering Congress and Exposition, Pittsburgh, PA, USA, 9–15 November 2018; pp. 1–10.
85. Tiari, S.; Rose, O.L.; Mahdavi, M. Discharging process of a high-temperature heat pipe-assisted thermal energy storage system with nano-enhanced phase change material. In Proceedings of the 4th Thermal and Fluids Engineering Conference (TFEC), Las Vegas, NV, USA, 14–17 April 2019; pp. 1–10.
86. Ren, Q.; Meng, F.; Guo, P. A comparative study of PCM melting process in a heat pipe-assisted LHTES unit enhanced with nanoparticles and metal foams by immersed boundary-lattice Boltzmann method at pore-scale. *Int. J. Heat Mass Transf.* **2018**, *121*, 1214–1228. [[CrossRef](#)]
87. Yu, J.; Yu, Z.C.; Tang, C.L.; Chen, X.; Song, Q.F.; Kong, L. Preparation and characterization of composite phase change materials containing nanoparticles. *Kemija U Industriji Časopis Kemičara I Kemijskih Inženjera Hrvatske* **2016**, *65*, 605–612. [[CrossRef](#)]
88. Senobar, H.; Aramesh, M.; Shabani, B. Nanoparticles and metal foams for heat transfer enhancement of phase change materials: A comparative experimental study. *J. Energy Storage* **2020**, *32*, 101911. [[CrossRef](#)]
89. Buonomo, B.; di Pasqua, A.; Ercole, D.; Manca, O. Numerical study of latent heat thermal energy storage enhancement by nano-PCM in aluminum foam. *Inventions* **2018**, *3*, 76. [[CrossRef](#)]
90. Ma, C.; Zhang, Y.; Chen, X.; Song, X.; Tang, K. Experimental study of an enhanced phase change material of paraffin/expanded graphite/nano-metal particles for a personal cooling system. *Materials* **2020**, *13*, 980. [[CrossRef](#)]
91. Kim, H.G.; Kim, Y.-S.; Kwac, L.K.; Shin, H.J.; Lee, S.O.; Lee, U.S.; Shin, H.K. Latent heat storage and thermal efficacy of carboxymethyl cellulose carbon foams containing Ag, Al, carbon nanotubes, and graphene in a phase change material. *Nanomaterials* **2019**, *9*, 158. [[CrossRef](#)] [[PubMed](#)]
92. Yu, Q.; Zhang, C.; Lu, Y.; Kong, Q.; Wei, H.; Yang, Y.; Gao, Q.; Wu, Y.; Sciacovelli, A. Comprehensive performance of composite phase change materials based on eutectic chloride with SiO₂ nanoparticles and expanded graphite for thermal energy storage system. *Renew. Energy* **2021**, *172*, 1120–1132. [[CrossRef](#)]
93. Mahdi, J.M.; Mohammed, H.I.; Hashim, E.T.; Talebizadehsardari, P.; Nsofor, E.C. Solidification enhancement with multiple PCMs, cascaded metal foam and nanoparticles in the shell-and-tube energy storage system. *Appl. Energy* **2020**, *257*, 113993. [[CrossRef](#)]